Modeling the Dynamics and Control of Lyme Disease in a Tick-Mouse System Subject to Vaccination of Mice Populations

Daniel Carrera-Pineyro[1], Harley Hanes[2], Adam Litzler[3], Andrea McCormack[4], Josean Velazquez-Molina[5], Christopher Kribs[6], Anuj Mubayi[5] and Karen R. Ríos-Soto[7]

[1]University of the Incarnate Word, San Antonio, Texas
[2]Tulane University, New Orleans, Louisiana
[3]The Ohio State University, Columbus, Ohio
[4]North Central College, Naperville, Illinois
[5]Arizona State University, Tempe, AZ
[6]The University of Texas at Arlington, Texas
[7]University of Puerto Rico at Mayagüez, Puerto Rico

Abstract

Lyme disease is one of the most prevalent and the fastest growing vector-borne bacterial illnesses in the United States, with over 25,000 new confirmed cases every year. Lyme disease cases have more than doubled in recent years, and the Centers for Disease Control and Prevention estimates that those numbers could be significantly underrepresented. Humans contract the bacteria, *Borrelia burgdorferi*, through the bite of *Ixodes scapularis*, commonly known as the deer tick or Eastern blacklegged tick. The tick can receive the bacterium from a variety of small mammal and bird species but *Peromyscus leucopus*, commonly known as white-footed mice, are the primary reservoirs in the northeastern United States, especially near human settlement. The life cycle and behavior of the ticks depends greatly on the season, with different stages of tick biting at different times. Reducing the infection in mice populations and the overall tick population may greatly reduce the number of humans affected by this disease in some parts of the affected region. However, research on the effects of various mouse-targeted interventions is limited. One particularly promising method is the administration of vaccine pellets to white-footed mice through special bait boxes. In this study, we develop and analyze a mathematical model consisting of a system of non-linear difference equations to understand the complex transmission dynamics and vector demographics in both tick and mice populations. Later, we evaluate to what extent vaccination of white-footed mice can affect the population of infected *I. scapularis* and under which conditions this method is a cost-effective preventative measure against Lyme disease. We find that vaccination can eliminate mouse=tick transmission of *B. burgdorferi* while saving money when instituted in areas with high human risk.

1 Introduction

Borrelia burgdorferi, a bacterial species of spirochete, is the main causative agent of Lyme disease, a tick-borne illness. The bacteria is mainly present in the northeastern United States, as well as

in areas of Asia and Europe [34]. In the U.S., there are approximately 30,000 confirmed cases reported to the Centers for Disease Control and Prevention (CDC) every year but actual cases have been estimated as high as 300,000 cases per year [11]. Symptoms can be debilitating, but may not appear for months after infection [12].

Lyme disease is transmitted only through the bite of various species of ticks. The bacteria is non-congenital; thus a parent cannot transmit the pathogen to its offspring simply by birth or nursing [20]. Reservoirs of *B. burgdorferi* include small mammals, such as mice, as well as some species of birds. Other animals which harbor the bacteria are shrews, chipmunks, and skunks. The focus of this research is to assess the effectiveness of a new control method for Lyme disease in the U.S.

1.1 Ecology of Mice and Ticks

In Eastern North America, the primary Lyme disease vector is the black-legged tick, *Ixodes scapularis*, also known as the deer tick. *I. scapularis* longevity can range from two to three years, and its life cycle is segmented into three stages as described in Figure 2. Ticks feed only three times in their lives, each time by taking a blood meal from a host. These blood meals are necessary for the tick to reach the next developmental life stage [12]. A tick feeds through a behavior known as questing, where it attaches with its posterior pair of legs to grass or short bushes and reaches out with its anterior pair for a host to graze against them [12]. The ticks then locate a suitable area to attach and feed from their host for three to five days [22]. *B. burgdorferi* can then enter the host through the tick's saliva while the tick feeds for the next 16 to 36 hours [7].

Black-legged ticks are born as susceptible larvae in the spring. In the following summer, they seek a blood meal from any sort of small mammal; this is where the ticks can initially become infected by feeding on an active reservoir. Afterwards they spend several days molting where they reach the nymphal stage and await the next spring. Nymphs feed on any size mammal, ranging from mice to deer to humans and tend to be predominantly active during the spring season [22]. This is where human risk is the greatest since nymphs are transparent in color and only about 2 millimeters in length, making them difficult to detect on the body. If the tick had previously become infected in the larval stage it can later, as a nymph, either reintroduce the bacteria into a susceptible mouse or infect a human. After molting again they reach the adult stage in the immediate fall and seek out a final blood meal. In the adult stage they prefer large mammals such as white tailed deer. Having completed their final blood meal in the fall, the adults mate, lay eggs, and then shortly die [17].

Although ticks will feed on a variety of hosts, of particular importance to the persistence of *B. burgdorferi* is the white-footed mouse *Peromyscus leucopus*. White-footed mice are the preferred biting targets of larval ticks and are often targeted by nymphs as well. These mice are generalist species who live in a variety of habitats in eastern North America. They especially thrive in habitats where their natural predators are absent, such as fragmented forests in and around suburban human settlements [39, 18]. *P. leucopus* do not experience any significant reduction in fitness due to either the *B. burgdorferi* bacteria or from feeding by larval and nymphal ticks. An individual mouse typically becomes infected by a nymphal tick, and goes on to spread the infection to many more larvae over the rest of its one-year life since a mouse may have up to 100 ticks in the larval and nymphal stages feeding on it at the same time [13]. These factors combined have all contributed

to the high prevalence of the disease in New England and the Upper Midwest.

It is important to note the seasonality in the tick activity: nymphs are mostly active in the spring, larvae in the summer, adults in the fall, and in the winter all stage activity decreases [17]. This is due to *I. scapularis*' behaviour being greatly sedentary and thus depend on their hosts as means of transportation. Since mice and deer activity tend to be lower during winter, so do tick bite rates in humans. Ticks in the United States do not have a natural predator, and winter is the only natural control mechanism. The advent of climate change leading to shorter, warmer winters is yet another factor in the proliferation of *I. scapularis* and *B. burgdorferi* throughout a widening range [25].

1.2 Previous Studies on Lyme Disease Transmission and Control

With the increase in tickborne diseases, much research has been undertaken in modeling transmission dynamics and understanding the impact of control methods [10, 14, 16, 32, 35]. Within the biology community there have been several studies of the potential for vaccines or acaricide, a poisonous substance for ticks and mites, as interventions to control transmission of *B. burgdorferi* between ticks and mice. Notable studies of vaccines include multiple lab studies showing efficacy of eliciting immune reactions in white-footed mice against *B. burgdorferi*'s OspA surface protein, thereby building resistance to infection in mice [8, 15, 35]. Additionally, field trials of vaccinating white-footed mice by distributing food with *E. coli* presenting *B. burgdorferi*'s OspA was effective at reducing prevalence of *B. burgdorferi* in both mice and nymphal ticks [29]. A current popular method of control is the use of bait boxes. Bait boxes are placed along frequented mice zones where the smell of food entices the mice to enter the box and pass through a wick covered in fipronil, a commonly used acaricide, which protects the mice from tick bites for the following 4 to 6 weeks [32]. A similar method was used in the distributions of vaccines for mice populations [32]. Many of these studies were conducted in fragmented forest environments. Forest fragmentation is a process where forests are reduced to small, disconnected patches called forest fragments. This phenomenon is a large threat to biodiversity since the area no longer becomes suitable to animals with larger ranges. White-footed mice, however, thrive in this kind of environment often completely out-compete other species of small mammal [18].

Other control methods to decrease infected ticks currently under investigation include introduction of other species as natural predators and control of mammalian host population. Most outsider species are not very effective at controlling tick populations with the exception of *Metarhizium anisopliae* fungus which is being tested to be sold for commercial use. Control of deer populations has not been shown to have a significant effect in reducing tick-borne diseases [16]. In this study we focus on modeling the introduction of orally induced vaccines into mice populations to determine the reduction of infected nymphal ticks and hence reduction in human cases.

Extensive modeling has been done by the mathematical community to try to understand the enzootic transmission cycle of *B. burgdorferi*. First among these are models that seek to understand the complex life cycle of *I. scapularis* and provide insight on factors affecting its behavior such as climate, host populations, and seasonal population dynamics [9, 24, 28]. Additionally, there has been extensive modeling of *B. burgdorferi* transmission that has given insight on its reproductive number with mice, the importance of targeting *I. scapularis* larvae, and the ability of *B.burgdorferi* to spread geographically [38, 40]. Our research advances this body of work by using the population

parameters and dynamics found in previous models, such as [2, 21, 23, 36], to model not just *B. burgdorferi*'s enzootic transmission, but leading efforts people can take to decrease transmission. This will provide critical insight to public health officials, researchers, and institutions seeking to assess the effectiveness of vaccines before they invest in their implementation and will also provide additional data to the small body of field trials that have been done.

In this research study, we model interacting tick and mouse populations subdivided into compartments based on infection stages for mice and infection status and life stage for ticks. We use a system of discrete difference equations for both populations to account for the seasonality in ticks. We first evaluate the model without vaccination to assess population dynamics and then with vaccination to determine its effectiveness on the population and estimate cost. Our aim is to model the populations in a fragmented forest environment in the Northeastern United States, where much of the field data is available and where human risk is especially high [34].

The next sections of this report will discuss how we obtained our model and equations. Following that is a section computationally analyzing the dynamics of the system and a cost-benefit analysis with regard to the total cost of Lyme disease treatment and prevention.

2 Methods

2.1 Model Development

In order to model the dynamics of infection between mice and ticks, we consider certain assumptions. The first is that there is homogeneous mixing between mice and ticks at all stages and that infection does not affect their movements or interactions within a certain geographical area. While we do account for mice having more contacts with larvae than nymphs, infected, vaccinated, and susceptible mice are all bitten by susceptible and infected ticks at equal constant rates. Additionally, we assume that infection with *B. burgdorferi* does not affect the birth or death rates of mice as well as the death or biting rates of ticks. We assume this because evidence suggests that *B. burgdorferi* does not cause any disease in ticks or white-footed mice, making them an excellent reservoir host [37]. The reproductive fitness of white-footed mice is also unaffected by the presence of the parasitic ticks [13].

We also assume that infectious mice and ticks remain infectious for the rest of their lives which is supported by current research on *B. burgdorferi* in *I. scapularis* and *P. leucopus* [4, 26, 33]. We assume that any larva or nymph that does not feed does not survive to feed in a later season or the next year which is true for the overwhelming majority of ticks [12]. This allows us to first compute death rates and declare that any larva or nymph that does not die must progress to nymph or adult, respectively. That is, we do not define an explicit rate at which ticks progress to the next stage in the life cycle without changing their infectivity; any ticks at a given stage which did not die or become infected must progress to the next stage with the same infectivity status. Another assumption in this model is that ticks are only infected by mice since white-footed mice have a very high population density and are the primary hosts of larvae [18]. White-footed mice also transmit and receive *B. burgdorferi* with greater effectiveness than other tick hosts, making them primary spreaders of the pathogen [5]. Another assumption about tick behavior in our model is that only one life stage of tick is feeding at a given time. Here, tick questing/feeding periods are mostly

divided into two separate seasons although in reality there is some overlap, particularly for nymphs and larvae, which will not be taken into account in this work. The final assumption of our model, for which there is scientific evidence, is that infected ticks and mice do not transmit *B. burgdorferi* to their offspring [20, 30].

2.2 Compartmental Model

For our model, we build a system of non-linear difference equations describing a susceptible, infectious, and vaccinated ($M_S - M_I - M_V$) mouse population coupled with a susceptible and infectious ($N_S - N_I$) tick population. To understand the mechanisms of these populations, life cycles, and infectiousness, we construct a compartmental diagram representing the dynamics of the system, capturing also the seasonality. We assume that the only species transmitting the infection are *I. scapularis* and *P. leucopus*. A flow chart capturing the dynamics of the system is shown below in Figure 1, and state variables and model parameters are summarized in Tables 1 and 2.

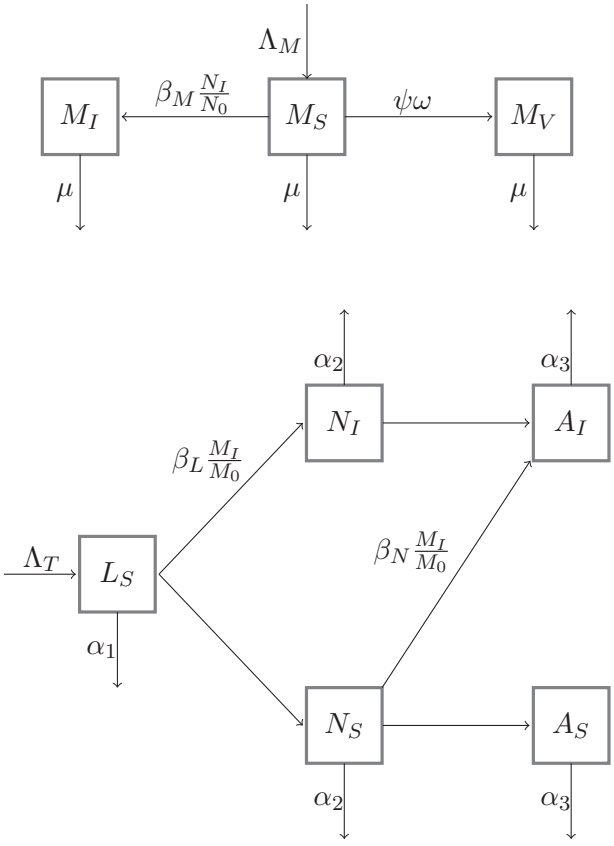

Figure 1: Mouse/Tick Compartmental Model

State Variables	Definition
$M(\tau+1)$	Total Mouse Population
$M_S(\tau+1)$	Susceptible Mice
$M_I(\tau+1)$	Infected Mice
$M_V(\tau+1)$	Vaccinated Mice
$L_S(\tau+1)$	Susceptible Larvae
$N(\tau+1)$	Total Nymph Population
$N_I(\tau+1)$	Infected Nymphs
$N_S(\tau+1)$	Susceptible Nymphs
$A_I(\tau+1)$	Infected Adults
$A_S(\tau+1)$	Susceptible Adults

Table 1: State Variables for Mice and Ticks, taken at time τ.

Parameter	Definition
Λ_M	Birth/recruitment of mice
β_M	Transmission constant from nymphs to mice
ψ	Contact between mice and vaccines
ω	Proportion of vaccine effectiveness
μ	Natural death of mice
Λ_T	Recruitment of larvae
β_L	Transmission constant from mice to larvae
β_N	Transmission constant from mice to nymphs
α_1	Egg to larva natural death
α_2	Larva to nymph natural death
α_3	Nymph to adult natural death

Table 2: Parameters for Population Dynamics

Mice have a constant birth Λ_M per generation and a uniform death rate μ, with a probability of survival given by $e^{-\mu}$. All mice are born as susceptible and can then become vaccinated with probability $e^{-\psi\omega}$, where ψ is the rate per year at which mice become vaccinated and ω the percent effectiveness of the vaccine. If not, they become infected by a nymphal tick with probability $e^{-\beta_M \frac{N_I}{N}}$, where β_M is a constant and $\frac{N_I}{N}$ weighs the impact of prevalence of nymphs infecting mice. $\beta_M \frac{N_I}{N}$ is dependent only on nymphs because we assume that larvae do not hatch being infected with *B. burgdorferi* so they cannot infect mice when they feed.

Ticks also have a constant recruitment per generation which is defined as Λ_T, being the number of larvae hatching every year. We assume a probability of death as $e^{-\alpha_i}$, with each α_i corresponding to a respective stage change's natural death as in Table 2. Larvae become infected with annual probability $e^{-\beta_L \frac{M_I}{M}}$, where β_L measures the impact of the bacteria infecting a susceptible larvae if it bites an infected mouse. Any larva that does not become infected or die progresses to a susceptible nymph. This transition is based on the assumption that no larvae survive through

the next summer without feeding and progressing to nymphs. Nymphs then begin feeding and susceptible nymphs can be infected with a probability of $e^{-\beta_N \frac{M_I}{M}}$, β_N is defined as the rate nymphs bite mice multiplied by the probability the bacteria infects a susceptible nymph if it bites an infected mouse. At this point infected nymphs that do not die can also feed on a susceptible mouse to infect it as is described in the mouse population. All infectious nymphs and susceptible nymphs that do not become infected adults become infectious and susceptible adults respectively. This transition is based on the assumption that no nymphs survive through the next spring without feeding and progressing to adults.

2.3 Seasonality

In order to derive the final model, we first divide a one year time-step into several subintervals, with each subinterval describing one specific process in the cycle. After each of the events is mathematically described, they can be chained together to describe the population dynamics from year to year. First, each important event in the system is associated with one or more arrows on the flowchart. The full list of these transition equations derived from these events is provided in Appendix 6.1.

For a visual representation of how the 2-year tick life cycle fits in to a model with 1-year time steps see Figure 2. Although there is only one generation and life stage assumed to be questing and feeding at a time, there are 2 generations that overlap each year. Our yearly cycle begins with nymphs in the spring which quest, feed, and begin molting to the adult phase. We then consider the larvae which hatch from the eggs of the previous year's adults and begin questing and feeding in the summer. These larvae will go on to become the next year's nymphs. In the summer those nymphs are dormant while they transition to adulthood and the larvae that hatched in the end of the spring begin questing and feeding. Those larvae molt during the fall and winter. In the fall, the adults, who were nymphs in the spring, lay the eggs for the next spring.

These building blocks are designed to be modular to allow for a possible different ordering of events. The system, for the purposes of this model, is approximated as happening in the following order: the cycle begins and ends in the spring, which is peak nymph activity. Thus the following sequence of events for the life cycle and infectiousness for the populations is considered:

Spring

1. Mice are vaccinated
   Mice are vaccinated at the beginning of our time-step because we want to measure the impact of vaccination as protection against nymphal ticks, thus vaccination must take place before nymphal ticks begin questing and feeding in the spring.

2. Susceptible mice become infected
   Mice being infected is the first event related to the nymphal feeding season. Larvae infected in the previous year have now progressed to nymphs and can infect mice by taking blood meals.

Summer

3. Nymphs become adults
   Nymphs becoming adults means that the nymph successfully feeds, and from there any of the following may occur:

   - Infected nymphs become infected adults (infected nymph potentially infects host)
   - Susceptible nymphs can become infected adults
   - Susceptible nymphs can become susceptible adults

4. Mice die
   Here we account for mice deaths that happen in the spring, after vaccination and after nymphs have fed. We separate this event from the other event of deaths in mice to account for the mice that are infected in the spring but do not survive to infect larvae in the summer.

5. Mice are born
   Here we account for new births in the mice population that happen in the spring after vaccination and the feeding of nymphs. We separate this event from the other event of births in mice so as to maintain a consistent population size after the deaths calculated in the previous step.

6. Larvae hatch
   Eggs hatch throughout the summer and become larvae. These larvae do not feed until the following spring (see Figure 2).

7. Larvae die
   Here we account for larval deaths that occur during the hatching season and while questing. Thus the future steps focusing on larvae can assume that all remaining larvae successfully feed.

8. Larvae feed on mice
   Here all remaining larvae successfully feed and become either infected or susceptible nymphs based on whether they feed on an infected mouse and receive the bacteria. In our model, we count these larvae as nymphs immediately after they feed whereas in reality they will not finish molting to nymphs until next spring.

   - Susceptible larvae can become susceptible nymphs
   - Susceptible larvae can become infected nymphs

Fall through end of winter

9. Nymphs die
   Here we account for all nymphs that died during molting or while questing. Thus the the solution for our nymph population is representative of the nymphs that successfully feed and progress to adult, rather than counting nymphs that would have died while molting.
   - Infected nymphs die
   - Susceptible nymphs die
10. Mice die
    Here we account for death that takes place from the beginning of summer until the end of spring so that our solution for mouse population is representative of the population at the beginning of spring.
11. Mice are born
    Here we account for birth that takes place from the beginning of summer until the end of spring so that our solution for mouse population is representative of the population at the beginning of spring.

In Figure 2, different generations are designated by the subscripts 0, 1, and 2. Generation 1 covers the two-year span of the image, Generation 0 finishes in fall of the first year, and Generation 0's descendants, Generation 2, begin their lives in summer of the second year. The subscripts are not the same as the τ-indexed yearly time steps in the model. The nymphs and adults for a particular year are the same generation of ticks, while the larvae are another. The vertical axis does not depict relative population size, but indicates respective seasons of questing individuals. In our model, the total population of any stage of tick in each year is the same as the total population of the same stage in every other year, which allows us to organize their two-year cycle in one year. This will be proved later in the analysis section.

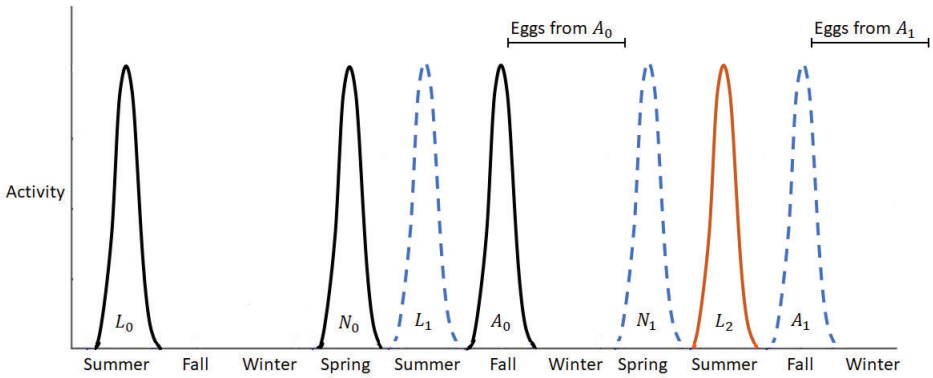

Figure 2: Tick life cycle.

2.4 Equations

To construct our system of equations, we use each rate on the flowchart to create an expression for population before and after its associated event, and then proceed by combining those equations into the full system. As an example, consider μ, the rate at which mice die. If we integrate to find the total population before and after one year's worth of deaths we get $M(\tau+1) = e^{-\mu}M(\tau)$. The proportion of mice that survive is $e^{-\mu}$. Likewise, the proportion of mice that die is $1-e^{-\mu}$.

To organize this ordering of events we separate the year into 11 sub-timesteps $\{\tau + \frac{i}{11} \mid i = 1,2,\ldots,11\}$. These sub-timesteps do not neccesarily correspond to a certain interval of time, and often we account for an entire year's worth of a particular process in each sub-step. If we wish to account for processes over only part of the year our proportions will be of the form $e^{-\zeta/k}$ for arbitrary parameter ζ and fraction of the year $1/k$. Furthermore, nonlinear terms will reference other state variables in the exponent, which introduces more complexity to the final equations. A full derivation of the system of equations can be found in Appendix 6.2.

The final system of equations (1), relating populations of mice and nymphs starting and ending during spring, is presented below. Adult and larvae stages are not included in these final populations as larvae have not yet hatched and adults died in the previous fall. However, the intermediate steps contain solutions for each stage at various points in the year.

Let $M(\tau) = M_S(\tau) + M_I(\tau) + M_V(\tau)$ and $N(\tau) = N_S(\tau) + N_I(\tau)$, the total population of mice and ticks, respectively. Then the system of equations, System (1), is given by:

$$N_I(\tau+1) = \Lambda_T e^{-\frac{(\alpha_1+3\alpha_2)}{4}} \left(1 - e^{-\frac{\beta_L}{4} \frac{M_I(\tau)e^{-\frac{\mu}{4}} + M_S(\tau)e^{-\frac{\mu}{4}}e^{-\frac{\psi\omega}{4}}\left(1-e^{-\frac{\beta_M}{2}\frac{N_I(\tau)}{N(\tau)}}\right)}{e^{-\frac{\mu}{4}}M(\tau) + \frac{\Lambda_M}{4}}} \right), \tag{1a}$$

$$N_S(\tau+1) = \Lambda_T e^{-\frac{(\alpha_1+3\alpha_2)}{4}} \left(e^{-\frac{\beta_L}{4} \frac{M_I(\tau)e^{-\frac{\mu}{4}} + M_S(\tau)e^{-\frac{\mu}{4}}e^{-\frac{\psi\omega}{4}}\left(1-e^{-\frac{\beta_M}{2}\frac{N_I(\tau)}{N(\tau)}}\right)}{e^{-\frac{\mu}{4}}M(\tau) + \frac{\Lambda_M}{4}}} \right). \tag{1b}$$

$$M_S(\tau+1) = M_S(\tau)e^{-\mu}e^{-\frac{\psi\omega}{4}}e^{-\frac{\beta_M}{2}\frac{N_I(\tau)}{N(\tau)}} + \frac{\Lambda_M}{4}(e^{-\frac{3\mu}{4}} + 3), \tag{1c}$$

$$M_I(\tau+1) = M_I(\tau)e^{-\mu} + M_S(\tau)e^{-\mu}e^{-\frac{\psi\omega}{4}}(1 - e^{-\frac{\beta_M}{2}\frac{N_I(\tau)}{N(\tau)}}), \tag{1d}$$

and

$$M_V(\tau+1) = M_V(\tau)e^{-\mu} + M_S(\tau)e^{-\mu}(1 - e^{-\frac{\psi\omega}{4}}). \tag{1e}$$

The number of susceptible mice at time $\tau+1$ is equal to the number of susceptible mice that did not die, did not become vaccinated, and did not become infected in the previous year plus the mice that were born - accounting for the fact that mice are born throughout the year by allowing 3/4 to be born before the larvae bite and 1/4 to be born after. The

number of infected mice at time $\tau + 1$ is equal to the number of infected mice that did not die plus the number of susceptible mice that became infected and did not die. Likewise, the number of vaccinated mice at time $\tau + 1$ is equal to the number of susceptible mice that did not die plus the number of susceptible mice that became vaccinated and did not die.

The number of infected and susceptible nymphs at time $\tau + 1$ is equal to the number of eggs hatched times the survival rate times the probability of becoming infected or not becoming infected, respectively. This rate is based on a contact rate times the proportion of all mice which were infected in the previous summer.

3 Mathematical Analysis

3.1 Total Populations of *I. scapularis* and *P. leucopus*

The total population size of mice can be described by calculating $M(\tau+1)$, the sum of the susceptible, infected, and vaccinated compartments at time $\tau + 1$. The value M_0 is the carrying capacity of mice in the system.

$$M(\tau + 1) = M_S(\tau + 1) + M_I(\tau + 1) + M_V(\tau + 1)$$
$$M(\tau + 1) = e^{-\mu} M(\tau) + \frac{\Lambda_M}{4} e^{\frac{-3\mu}{4}} + \frac{3}{4}\Lambda_M$$

This is a linear difference equation whose solution is:

$$\begin{aligned} M(\tau) &= M(0)(e^{-\mu})^\tau + \frac{\Lambda_M}{4}(e^{-\frac{3\mu}{4}} + 3)\sum_{i=0}^{\tau-1} e^{-\mu i} \\ &= M(0)(e^{-\mu})^\tau + \frac{\Lambda_M}{4}(e^{\frac{-3\mu}{4}} + 3)\left(\frac{1 - (e^{-\mu})^\tau}{1 - e^{-\mu}}\right) \end{aligned}$$

Since μ is a positive constant, $e^{-\mu}$ is a proportion and $0 < e^{-\mu} < 1$. Therefore:

$$\lim_{\tau\to\infty} M(\tau) = \frac{\Lambda_M}{4}\frac{(e^{-\frac{3\mu}{4}} + 3)}{1 - e^{-\mu}} = M_0$$

This is the mouse population at demographic steady state, and it can also be written as:

$$M_0 = \frac{\Lambda_M}{4} e^{-3\mu/4}\frac{1}{1 - e^{-\mu}} + \frac{3\Lambda_M}{4}\frac{1}{1 - e^{-\mu}} = M_0^1 + M_0^2$$

In biological terms, it is the number of mice born during event 5 of any year that did not die plus the number of mice born during event 11 of any year.

Similar calculations can be performed on the total nymphal tick population with $N(\tau + 1)$ equal to the sum of the susceptible and infected tick populations at time τ. In the construction of this model, we assumed that there are no demographic pressures on the population other than the

constant birth and death rates, so $N(\tau)$ is constant from year to year as well. That is,

$$N(\tau+1) = N_S(\tau+1) + N_I(\tau+1) = \Lambda_T e^{-\frac{(\alpha_1+3\alpha_2)}{4}}$$

thus,

$$N_0 = \Lambda_T e^{-\frac{(\alpha_1+3\alpha_2)}{4}} \text{ for all time } \tau.$$

The total nymph population is equal to the number of hatched eggs times the proportion of nymphs that do survive before the sampling time. It follows from this calculation of M_0 and N_0 that we can reduce System (1) to a system of three equations. Let $M_S(\tau) = M_0 - (M_I(\tau) + M_V(\tau))$ and $N_S(\tau) = N_0 - N_I(\tau)$. The system becomes System (2), which is only in terms of the N_I, M_I, and M_V populations. System (2) will be used throughout the rest of the paper, including in the numerical simulations (Section 4), and is given by:

$$N_I(\tau+1) = \Lambda_T e^{-\frac{(\alpha_1+3\alpha_2)}{4}} \left(1 - e^{-\frac{\beta_L}{4} \frac{M_I(\tau)e^{-\frac{\mu}{4}} + (M_0 - M_I(\tau) - M_V(\tau))e^{-\frac{\mu}{4}} e^{-\frac{\psi\omega}{4}} \left(1 - e^{-\frac{\beta_M}{2}\frac{N_I(\tau)}{N_0}}\right)}{e^{-\frac{\mu}{4}} M_0 + \frac{\Lambda_M}{4}}} \right), \quad \text{(2a)}$$

$$M_I(\tau+1) = M_I(\tau)e^{-\mu} + (M_0 - M_I(\tau) - M_V(\tau))\, e^{-\mu} e^{-\frac{\psi\omega}{4}} (1 - e^{-\frac{\beta_M}{2}\frac{N_I(\tau)}{N(\tau)}}), \quad \text{(2b)}$$

$$M_V(\tau+1) = M_V(\tau)e^{-\mu} + (M_0 - M_I(\tau) - M_V(\tau))\, e^{-\mu} (1 - e^{-\frac{\psi\omega}{4}}). \quad \text{(2c)}$$

In the next section we proceed to calculate the fixed points of System (2)in order to understand its long-term dynamics.

3.2 Fixed Points of System (2)

To find fixed points, we start by setting the equations in System (2) equal to their respective populations. That is,

$$N_I(\tau+1) = N_I(\tau) = N_I^*,$$
$$M_I(\tau+1) = M_I(\tau) = M_I^*,$$
and
$$M_V(\tau+1) = M_V(\tau) = M_M^*.$$

The disease-free equilibrium is obtained by letting $N_I^* = 0$, $(N_S^*, N_I^*, M_S^*, M_I^*, M_V^*)$ where each of the entries are given by:

$$
\begin{aligned}
N_S^* &= N_0, \\
N_I^* &= 0, \\
M_S^* &= M_0 \frac{1-e^{-\mu}}{1-e^{-\mu-\frac{\psi\omega}{4}}}, \\
M_I^* &= 0, \\
&\text{and} \\
M_V^* &= M_0 \frac{e^{-\mu}(1-e^{-\frac{\psi\omega}{4}})}{1-e^{-\mu-\frac{\psi\omega}{4}}}.
\end{aligned}
$$

As expected, the total population is at demographic steady state; $M_S^* + M_V^* = M_0$. We can also interpret the mouse populations at disease-free equilibrium as proportions of the total equilibrium mouse population. That is,

$$
\begin{aligned}
\frac{M_S^*}{M_0} &= \frac{1-e^{-\mu}}{1-e^{-\mu-\frac{\psi\omega}{4}}}, \\
&\text{and} \\
\frac{M_V^*}{M_0} &= \frac{e^{-\mu}(1-e^{-\frac{\psi\omega}{4}})}{1-e^{-\mu-\frac{\psi\omega}{4}}}.
\end{aligned}
$$

The expression $\frac{M_S^*}{M_0}$ is the proportion of mice that die and are thus replaced at demographic equilibrium over the proportion that either get vaccinated or die. Furthermore, $\frac{M_V^*}{M_0}$ is the proportion that survive times the proportion that do get vaccinated over the proportion that either die or get vaccinated.

3.3 Stability of the Disease-Free Equilibrium and Calculation of $\mathcal{R}_C$, the Control Reproduction Number

The stability of the disease-free equilibrium can be achieved by linearizing System (2) and calculating the Jacobian at the disease-free equilibrium and through the eigenvalues. Notice that this matrix is singular; the first row is a constant multiple $\frac{e^{-\frac{(\alpha_1+3\alpha_2)}{4}}\left(1-e^{-\mu}\right)\beta_L\Lambda_T}{\left(3e^{-\mu}+e^{-3\mu/4}\right)\Lambda_M}$ of the second. The Jacobian matrix of System (2) is given by

$$
J(N_I^*, M_I^*, M_V^*) = \begin{bmatrix}
\frac{\partial N_I(\tau+1)}{\partial N_I(\tau)} & \frac{\partial N_I(\tau+1)}{\partial M_I(\tau)} & \frac{\partial N_I(\tau+1)}{\partial M_V(\tau)} \\
\frac{\partial M_I(\tau+1)}{\partial N_I(\tau)} & \frac{\partial M_I(\tau+1)}{\partial M_I(\tau)} & \frac{\partial M_I(\tau+1)}{\partial M_V(\tau)} \\
\frac{\partial M_V(\tau+1)}{\partial N_I(\tau)} & \frac{\partial M_V(\tau+1)}{\partial M_I(\tau)} & \frac{\partial M_V(\tau+1)}{\partial M_V(\tau)}
\end{bmatrix},
$$

$J(N_I^*, M_I^*, M_V^*)\big|_{D.F.E} =$

$$\begin{bmatrix} \frac{\beta_M\beta_L}{8}\frac{(3e^{-\frac{\mu}{4}}+e^{-\mu})e^{-\frac{3\mu}{4}-\frac{\psi\omega}{4}}}{(1-e^{-\mu-\frac{\psi\omega}{4}})}\frac{\left(1-e^{-\mu}\right)}{\left(3e^{-\mu}+e^{-3\mu/4}\right)} & e^{-\mu}\frac{e^{-\frac{(\alpha_1+3\alpha_2)}{4}}\left(1-e^{-\mu}\right)\beta_L\Lambda_T}{\left(3e^{-\mu}+e^{-3\mu/4}\right)\Lambda_M} & 0 \\ \frac{\beta_M\Lambda_M}{8\Lambda_T}\frac{(3e^{-\frac{\mu}{4}}+e^{-\mu})e^{-\frac{3\mu}{4}-\frac{\psi\omega}{4}}}{(1-e^{-\mu-\frac{\psi\omega}{4}})e^{-\frac{(\alpha_1+3\alpha_2)}{4}}} & e^{-\mu} & 0 \\ 0 & -e^{-\mu}\left(1-e^{-\frac{\psi\omega}{4}}\right) & e^{-\mu-\frac{\psi\omega}{4}} \end{bmatrix}.$$

The eigenvalues of the Jacobian matrix evaluated at the D.F.E. are:

$$\begin{aligned} &\lambda_1 = 0, \\ &\lambda_2 = e^{-\mu-\frac{\psi\omega}{4}}, \\ &\text{and} \\ &\lambda_3 = e^{-\mu} + \frac{\beta_M}{2}\frac{\beta_L}{4}\left(\frac{1-e^{-\mu}}{1-e^{-\mu-\frac{\psi\omega}{4}}}\right)\left(\frac{e^{-\mu}+3e^{\frac{-\mu}{4}}}{e^{\frac{-3\mu}{4}}+3e^{-\mu}}\right)e^{\frac{-3\mu}{4}-\frac{\psi\omega}{4}}. \end{aligned}$$

The first two eigenvalues λ_1 and λ_2 both have magnitude less than 1. The third eigenvalue may or may not be less than 1 in magnitude, and it therefore serves as a condition for stability. If $|\lambda_3| < 1$, the disease-free equilibrium is locally stable. Otherwise, it is unstable. However, since all of the parameters are defined as positive constants, λ_3 is strictly positive, meaning we can reduce the expression further.

$$\begin{aligned} &e^{-\mu} + \frac{\beta_M}{2}\frac{\beta_L}{4}\left(\frac{1-e^{-\mu}}{1-e^{-\mu-\frac{\psi\omega}{4}}}\right)\left(\frac{e^{-\mu}+3e^{\frac{-\mu}{4}}}{e^{\frac{-3\mu}{4}}+3e^{-\mu}}\right)e^{\frac{-3\mu}{4}-\frac{\psi\omega}{4}} < 1 \\ \iff &\frac{\beta_M}{2}\frac{\beta_L}{4}\left(\frac{1-e^{-\mu}}{1-e^{-\mu-\frac{\psi\omega}{4}}}\right)\left(\frac{e^{-\mu}+3e^{\frac{-\mu}{4}}}{e^{\frac{-3\mu}{4}}+3e^{-\mu}}\right)e^{\frac{-3\mu}{4}-\frac{\psi\omega}{4}} < 1-e^{-\mu} \\ \iff &\frac{\beta_M}{2}\frac{\beta_L}{4}\left(\frac{1}{1-e^{-\mu-\frac{\psi\omega}{4}}}\right)\left(\frac{e^{-\mu}+3e^{\frac{-\mu}{4}}}{e^{\frac{-3\mu}{4}}+3e^{-\mu}}\right)e^{\frac{-3\mu}{4}-\frac{\psi\omega}{4}} < 1. \end{aligned}$$

Therefore, let

$$r = \left(\frac{\beta_M\beta_L}{8(1-e^{-\mu-\frac{\psi\omega}{4}})}\right)\left(\frac{e^{-\mu}+3e^{\frac{-\mu}{4}}}{e^{\frac{-3\mu}{4}}+3e^{-\mu}}\right)e^{\frac{-3\mu}{4}-\frac{\psi\omega}{4}}. \tag{3}$$

Although $r < 1$ is a condition for stability, $r \neq \mathcal{R}_C$. But by Allen and van den Driessche [3] either $r = \mathcal{R}_C = 1$, $1 < r \leq \mathcal{R}_C$, or $0 \leq \mathcal{R}_C \leq r < 1$, meaning stability conditions based on r are equivalent to stability conditions based on $\mathcal{R}_C$. The canonical value of $\mathcal{R}_C$ can be calculated using the next-generation matrix approach. We begin by representing the Jacobian matrix as follows:

$$J = \begin{bmatrix} F+T & \mathcal{O} \\ A & C \end{bmatrix}$$

where $F + T$ is the 2×2 submatrix relating the N_I and M_I compartments, $\mathcal{O}$ is the 2×1 zero

matrix, A is a 1×2 matrix, and C is the 1×1 matrix $\left[e^{-\mu-\frac{\psi\omega}{4}}\right]$. F consists of all terms relating to new infections and T consists of all other terms in each matrix entry.

$$F = \begin{bmatrix} \frac{\beta_M \Lambda_M}{8\Lambda_T} \frac{(3e^{-\frac{\mu}{4}}+e^{-\mu})e^{-\frac{3\mu}{4}-\frac{\psi\omega}{4}}}{(1-e^{-\mu-\frac{\psi\omega}{4}})e^{-\frac{(\alpha_1+3\alpha_2)}{4}}} & \frac{e^{-\frac{(\alpha_1+3\alpha_2)}{4}}\left(1-e^{-\mu}\right)\beta_L\Lambda_T}{\left(3e^{-\mu}+e^{-3\mu/4}\right)\Lambda_M} & e^{-\mu}\frac{e^{-\frac{(\alpha_1+3\alpha_2)}{4}}\left(1-e^{-\mu}\right)\beta_L\Lambda_T}{\left(3e^{-\mu}+e^{-3\mu/4}\right)\Lambda_M} \\ \frac{\beta_M \Lambda_M}{8\Lambda_T} \frac{(3e^{-\frac{\mu}{4}}+e^{-\mu})e^{-\frac{3\mu}{4}-\frac{\psi\omega}{4}}}{(1-e^{-\mu-\frac{\psi\omega}{4}})e^{-\frac{(\alpha_1+3\alpha_2)}{4}}} & & 0 \end{bmatrix}$$

and

$$T = \begin{bmatrix} 0 & 0 \\ 0 & e^{-\mu} \end{bmatrix}.$$

As with the full Jacobian, the matrix F+T is singular as well. We can also use r from above to simplify this calculation. Let $F = \left(\begin{smallmatrix} ka & kb \\ a & 0 \end{smallmatrix}\right)$ and $T = \left(\begin{smallmatrix} 0 & 0 \\ 0 & b \end{smallmatrix}\right)$ We can use these matrices to calculate the next-generation matrix Q and an expression for $\mathcal{R}_C$.

$$\begin{aligned} Q &= F(I_{2\times 2} - T)^{-1} \\ &= \begin{bmatrix} ka & \frac{kb}{1-b} \\ a & 0 \end{bmatrix}, \end{aligned}$$

with the associated eigenvalues,

$$\lambda_{1,2} = \left\{ \frac{1}{2}\left(ka \pm \sqrt{(ka)^2 + \frac{4(ka)b}{1-b}} \right) \right\},$$

in which case,

$$\begin{aligned} \mathcal{R}_C &= \frac{1}{2}\left(ka + \sqrt{(ka)^2 + \frac{4(ka)b}{1-b}} \right) \\ &= \frac{1}{2}\left(\frac{\left(1-e^{-\mu}\right)\left(e^{-\mu}+3e^{-\mu/4}\right)\beta_L\beta_M e^{-\frac{3\mu}{4}-\frac{\psi\omega}{4}}}{8\left(3e^{-\mu}+e^{-3\mu/4}\right)\left(1-e^{-\mu-\frac{\psi\omega}{4}}\right)} \right) + \\ &\frac{1}{2}\sqrt{\frac{\left(1-e^{-\mu}\right)^2\left(e^{-\mu}+3e^{-\mu/4}\right)^2\beta_L^2\beta_M^2 e^{-\frac{3\mu}{2}-\frac{\psi\omega}{2}}}{64\left(3e^{-\mu}+e^{-3\mu/4}\right)^2\left(1-e^{-\mu-\frac{\psi\omega}{4}}\right)^2} + \frac{\left(e^{-\mu}+3e^{-\mu/4}\right)\beta_L\beta_M e^{-\frac{7\mu}{4}-\frac{\psi\omega}{4}}}{2\left(3e^{-\mu}+e^{-3\mu/4}\right)\left(1-e^{-\mu-\frac{\psi\omega}{4}}\right)}} \end{aligned}$$

This depends on $\frac{\partial N_I(\tau+1)}{\partial N_I(\tau)}$ and a term representing $\frac{\partial N_I(\tau+1)}{\partial N_I(\tau)}$ times $\frac{b}{1-b}$, the total mice that have survived to year τ. Since $e^{-\mu-\frac{\psi\omega}{4}}$, the spectral radius of C, is always between 0 and 1, $\mathcal{R}_C$ provides a stability condition for the disease-free equilibrium. If $\mathcal{R}_C < 1$, the equilibrium is stable. Otherwise, it is unstable.

3.4 Existence of Endemic Equilibria

To prove the existence of fixed points we reduce this system to one equation. We solve Equation (2c) in terms of M_I^* and Equation (2b) in terms of N_I^*. Plugging those two equations into Equation (2a) we can write a single equation in terms of N_I^*. For the full derivation, see Appendix 6.4. The number of roots of this equation will determine the number of solutions, and is given by:

$$G(N_I^*) = \ln\left(1 - \frac{N_I^*}{N_0}\right) + \frac{\beta_L M_0 e^{-\frac{\mu}{4}} e^{-\frac{\psi\omega}{4}}}{4\left(e^{\frac{-\mu}{4}} M_0 + \frac{\Lambda_M}{4}\right)} \left(\frac{1 - e^{\frac{-\beta_M}{2}\frac{N_I^*}{N_0}}}{1 - e^{-\mu} e^{\frac{-\psi\omega}{4}} e^{\frac{-\beta_M}{2}\frac{N_I^*}{N_0}}}\right) = 0. \tag{5}$$

Since this equation is transcendental, we can not analytically find zeros of Equation (5). However, by inspection, we notice that $G(0) = 0$, which suggests the existence of a disease-free equilibrium. We can find other roots numerically by graphing the equation with the parameter values found in the literature. Because of the large range of available estimates for contact rates β_L and β_N we plot three curves, one for each parameter value chosen. For a more detailed explanation of these estimates see Section 4.1. The beta values in Figure 3, are listed per year and correspond to values of low contact, medium contact, and high contact from bottom to top.

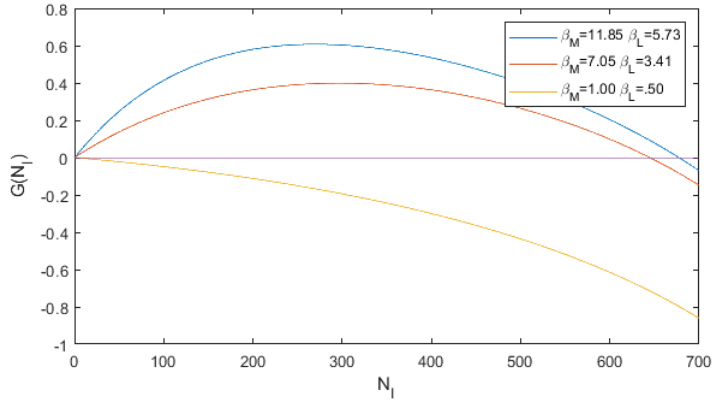

Figure 3: Existence of equilibrium with vaccination. Equilibria correspond to roots of G.

In Figure 3, it is evident that, for medium and high contact rates there exist two solutions: the disease-free and the endemic equilibrium. The graph demonstrates a parabolic behavior having a root at $G(0) = 0$, reaching a max and then going downwards until it reaches another root. Therefore we know that there exists at least one positive root by the Intermediate Value Theorem by observing the positive values in the graph for $N_I > 0$ and knowing $\lim_{N_I \to \infty} G(N_I) = -\infty$. For the low contact rates, $\beta_M = 1$ and β_L=0.5, we notice different behavior. $G`(N_I) < 0$ for all N_I, and the only non-negative root is $N_I* = 0$. In fact, in this low contact rate scenario, we can calculate that $\mathcal{R}_C < 1$, meaning that the disease-free equilibrium is stable.

4 Numerical Results

4.1 Parameter Estimation

Parameter	Definition	Value	Units	Reference
M	Total mouse population	50	Individuals	[21]
Λ_M	Birth/recruitment of mice	65.02	Individuals	
ψ	Contact between mice and vaccines	Estimated	1/year	
β_M	Transmission from nymphs to mice	Estimated	1/year	
ω	Proportion of vaccine effectiveness	0.96	1/year	[35]
μ	Natural death rate of mice	4.38	1/year	[23, 38]
N	Total nymph population	1000	Individuals	[2]
Λ_T	Recruitment of larvae	$1.998\text{x}10^5$	Individuals	
β_L	Transmission from mice to larvae	Estimated	1/year	
β_N	Transmission from mice to nymphs	Estimated	1/year	
α_1	Egg to larva natural death	11.98	1/year	[36]
α_2	Larva to nymph natural death	3.07	1/year	[36]
α_3	Nymph adult natural death	3.22	1/year	[36]

Table 3: Parameters values for population dynamics

Many of these parameters are given as rates in units of 1/year, which were often converted from 1/day as found in literature. Whenever these parameters appear in the model they are always within exponents, e.g. $e^{-\mu}$, which converts the rates into proportions as is necessary for the discrete-time model. Our time step of one year is subdivided by seasons in order to accurately account for tick life/activity stages, thus some of the proportions are shown to be fractions. For example, $e^{\frac{-3\mu}{4}}$ represents the survival for three out of the four seasons. This use of fractional exponents is used for recruitment, death, vaccination, and contact constants.

Values for α_1, α_2, and α_3 were derived from survival proportions between each stage of the tick life cycle; exact calculations are in Appendix 6.5. The total mouse population of 50 and total nymph population of 1000 were estimated using data on mice and tick populations in fragmented forest areas, relating woodland size to population density. We focused on plot sizes of 1.1 hectares to match the study that gave us our proportion of vaccine effectiveness [35]. Though the data varied, we chose populations that had biological significance and would allow us to simulate our model. Values Λ_M and Λ_T were calculated from the population death rates and sizes, using the equilibrium solutions for the total mouse and tick populations as found in Appendix 6.2. The three sets of β values in units of 1/year, β_N= 0.68, 0.86, and 1.47, β_L=3.41, 4.29, and 5.73, and β_M=7.05, 8.87, and 11.85, were estimated to signify very low, moderate, and high transmission rates, each respectively corresponding to approximately 20%, 35% and 50% of nymphs infected at equilibrium. Since biting rates between ticks and mice are dependent on abiotic factors and proportions of other nymph hosts that are not present in our model, we wanted to use β values that would provide information on a wide range of biologically feasible scenarios. All calculations for parameter values are explained further in Appendix 6.5.

4.2 Numerical Analysis

Below is a directory for all of the simulations conducted in this section.

Scenario	Figures	Summary	Parameters
1	4	Simulate susceptible, infected, and vaccinated populations vs time to understand general trends.	β_N=0.86/yr, β_L=4.29/yr, β_M= 8.87/yr, $\mathcal{R}_C = 1.27$
2	5	Vary contact rates β_N, β_L, and β_M; find equilibrium infectious proportions and $\mathcal{R}_0$ with no vaccination.	$\psi = 0$
3	6, 7, 8	Vary vaccination rate with fixed contact rates; find equilibrium infectious proportions.	Figure 6: low contact rates, $\mathcal{R}_C \in [0.18, 3.02]$. Figure 7: medium contact rates, $\mathcal{R}_C \in [0.28, 4.77]$. Figure 8: high contact rates, $\mathcal{R}_C \in [0.48, 8.51]$.
4	9	Vary vaccination rate to find $\mathcal{R}_C$.	Low, medium, and high contact rates for moderate transmission
5	10	Vary vaccination rate to find infectious proportions after 2, 5, and 10 years.	Low, medium, and high contact rates

The first step in numerical analysis was creating plots of mouse and tick populations with respect to time to confirm the equations behaved as hypothesized. These simulations were implemented using MATLAB. These results were surprising in that populations tended to reach equilibrium within the first 6 years. However, vaccination's ability to drive an endemic equilibrium with a high proportion of infected ticks to one with very few infected ticks was as expected.

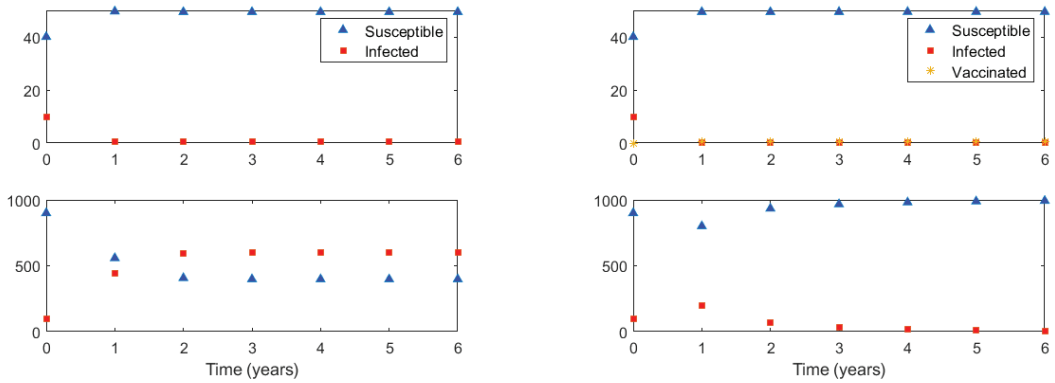

(a) No Vaccination (b) Vaccination

Figure 4: Mouse and nymph populations with and without vaccination at M=50 mice, N=1000 ticks, β_N=0.86/year, β_L=4.29/year, β_M=8.87/year, $\mathcal{R}_C = 1.27$, $\mathcal{R}_0 = 4.77$.

The next step in our analysis was to measure the change in the asymptotic equilibrium for increasing infectious contact rates. We vary infectious contact rates by keeping a constant ratio between β_N, β_L, and β_M, varying their magnitude as seen in Figure 5. There is a set ratio between the mouse and the nymphal contact rate because they are both dependent on the rate at which ticks bite mite. To convert the tick biting rate to the mouse biting rate, we multiplied by the proportion of nymphs to mice. We set β_N to vary from 0 to 1.2 and then tested varying ratios between β_N and β_L until we found sets of contact rates that corresponded to percent nymphs infected at equilibrium that matched biological expectations[29]. For this simulation we keep $\psi = 0$ which represents no vaccination. This was critical to providing estimates for contact rates but also revealed novel dynamics. The mouse population asymptotically approaches approximately 1.2% infected as contact rates increase. This can be explained by the ordering of events in our model, specifically observing that three-fourths of mice recruitment takes place at the end of the year. Since all mice are born susceptible, these mice are counted as susceptible at our sampling time in the next spring. Even if 100% of mice were to be infected after the nymph biting period, those mice must survive fall, winter, and most of spring to affect the next cycle, which gives biological justification to the trend in Figure 5 explained above. Due to the short life span of the mice, only a very low proportion of them actually make it to the next spring, so biologically there should always be a minimum number of susceptible mice in the spring.

Another important finding of these simulations is that mice almost immediately reach the threshold of infected mice (for a value of β_L=4) while the proportion of infected nymphs is still approximately 30%. This means that the spring population of mice is not a good predictor of the proportion of infected nymphs that year as the percent of nymphs infected could vary from 30% to 100% with very little measurable change in mouse infection prevalence. Additionally, the infected mouse population is so small for any infectious contact rates that any field estimation would be very difficult. In short, while the exact maximum proportion of infected mice will vary between geographical regions and mice habitats, the proportion of infected mice measured it in the spring is not a good predictor for Lyme disease risk that year. This simulation also confirms the stability of a disease free equilibrium when $\mathcal{R}_C < 1$ for values of β_L below 2.75 (see Figure 5).

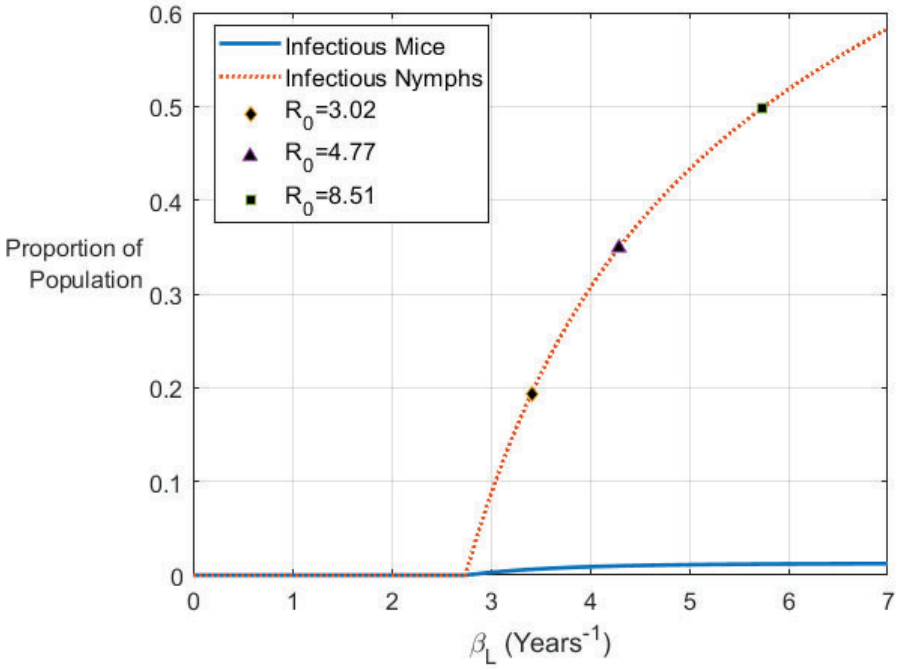

Figure 5: Asymptotic fixed points for infected mice and nymph proportions of population as β_L varies, M=50, N=1000, $\psi = 0$, R_0=[0, 12.68].

We now analyze the asymptotic behavior of endemic equilibria with respect to varying vaccination rates, ψ, at the low (Figure 6), medium (Figure 7), and high (Figure 8) test values for contact rates between mice and ticks as discussed in our parameter estimation. These plots show that the proportion of infected ticks can be reduced to less than one (less than 10^{-3} proportion infected since the nymphal population size is 1000) at vaccination rates of approximately 2/year, 4/year, and 6/year[1] for the low, medium, and high sets of infectious contact rates values respectively. This shows an approximately linear relationship between an endemic equilibrium of ticks infected without vaccination and the vaccination rate required to control the epidemic. If equilibrium infection prevalence increases by 15% then the vaccination rate required to eliminate the pathogen is an additional 2/year. For example, the low set of contact rates which correspond to approximately 20% of nymphs infected require a vaccination rate of 2/year to be reduced to less than one infected tick (Figure 6). The medium contact rates which correspond to approximately 35% infected require a vaccination rate of 4/year to be reduced to less than one infected tick (Figure 7). A similar change is seen again from the medium contact rates to the high contact rates, corresponding to 50% of nymphs infected, as they require a vaccination rate of 6 per year to be reduced to less than one infected nymph (Figure 8). This can be a guide to those seeking to introduce vaccination across a variety of areas who may not have the aid of computational tools to recalculate vaccination rates for each area.

[1]A note on interpretation: A vaccination rate of $\psi = 6$/year means it takes one mouse an average of 1/6 of a year to encounter a bait box.

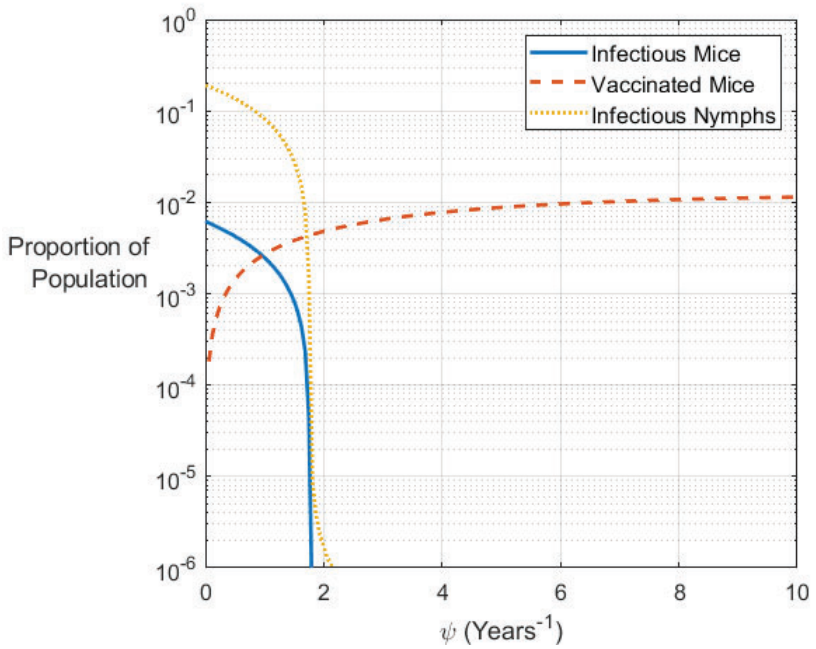

Figure 6: Population proportions at low contact rates as ψ varies at M=50, N=1000 $\beta_N = 0.68$/year, $\beta_L = 3.41$/year, $\beta_M = 7.05$/year, $\mathcal{R}_C = [0.18, 3.02]$.

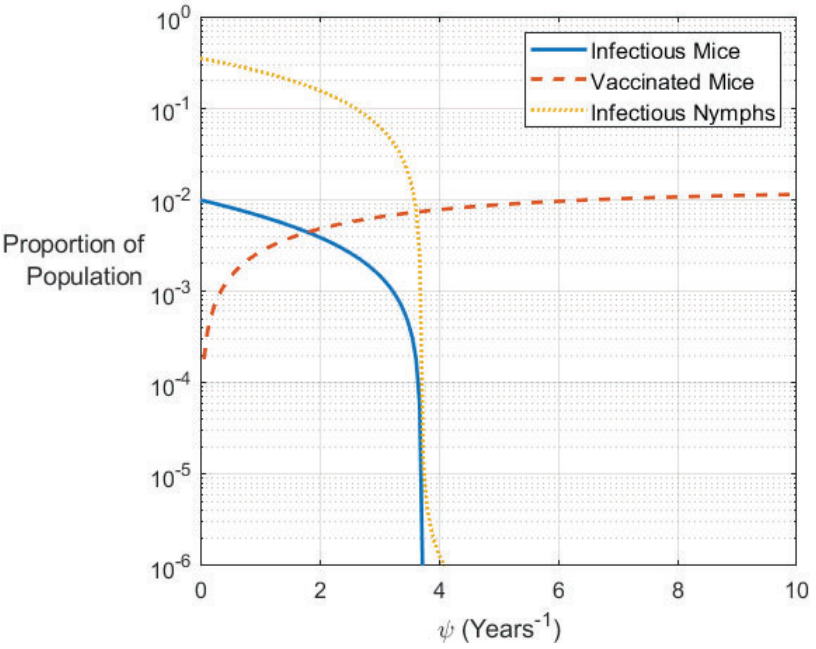

Figure 7: Population proportions at medium contact rates as ψ varies at M=50, N=1000 $\beta_N = 0.86$/year, $\beta_L = 4.29$/year, $\beta_M = 8.87$/year, $\mathcal{R}_C = [0.28, 4.77]$.

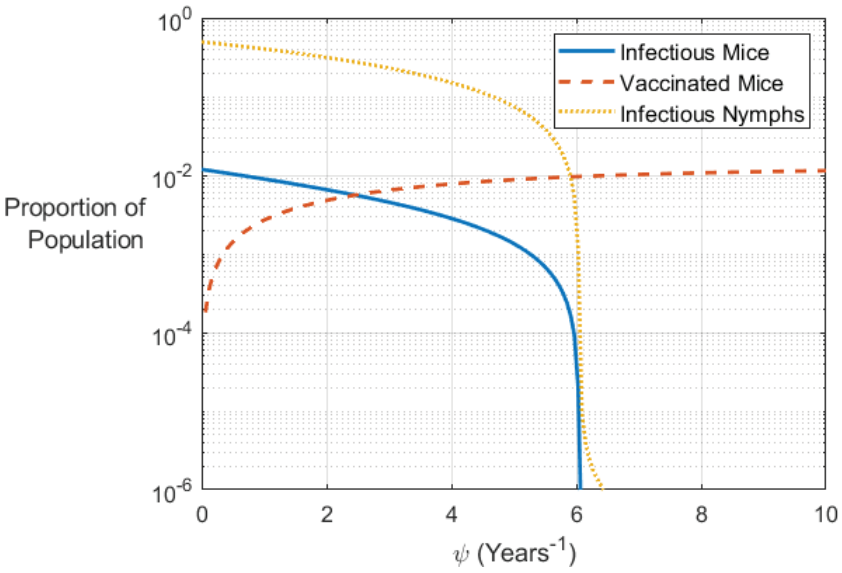

Figure 8: Population proportions at high contact rates as ψ varies at M=50, N=1000 $\beta_N = 1.47$/year, $\beta_L = 5.73$/year, $\beta_M = 11.85$/year, $\mathcal{R}_C = [0.48, 8.51]$.

We also wish to know at which values of ψ the disease-free equilibrium is stable. So in Figure 9 we plot $\mathcal{R}_C$ vs ψ for the same three sets of infectious contact rates as in Figures 6, 7, and 8. In Figure 9, the point where any of the curves cross the line $\mathcal{R}_C = 1$ (10^0) is the critical point in determining the stability. For small β values, this is at $\psi = 4.58$/year, for medium β values, it is at $\psi = 6.55$/year, and at large β values, this is at $\psi = 11.04$/year. As expected, higher transmission rates lead to a greater $\mathcal{R}_C$ and more vaccination is needed to bring the epidemic under control. Important to note is that the vaccination rates required to reduce the proportion of infected ticks to less than 1 are significantly less than the vaccination rates required to reduce $\mathcal{R}_C$ to less than 1. The difference between these interpretations is that numerically there exist endemic equilibria with the number of infected ticks between 0 to 1, however, these values do not make sense biologically since fractional ticks do not exist. This implies that, though $\mathcal{R}_C$ is a sufficient condition for elimination of *B. burgdorferi* in the mouse-tick system, it is not a necessary condition, so analysis of vaccine effectiveness should not center on $\mathcal{R}_C$.

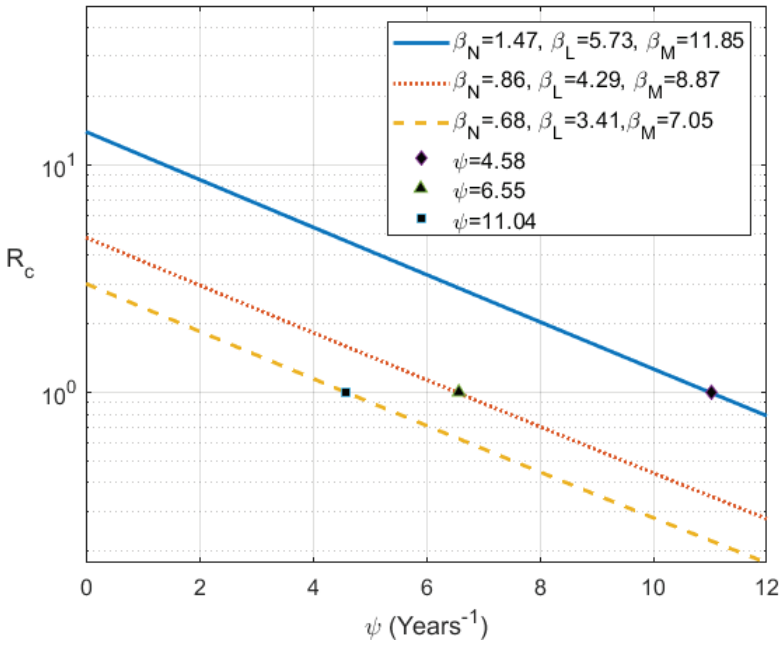

Figure 9: $\mathcal{R}_C$ vs ψ at varying values of β

Mapping equilibria as done in Figures 6, 7, and 8 is not necessarily feasible for determining usefulness of an intervention since results are often expected much sooner than equilibria occur. Therefore, we also mapped the effect of vaccination on the proportion of infected nymphs after two, five, and ten years in Figure 10. These results showed that, not only can vaccinating mice significantly reduce the endemic prevalence, it can do so within short time periods. Vaccination was effective at reducing the number of infected nymphs to zero for all infectious contact rates within the range of vaccination rates sampled. The number of infected ticks at the different time intervals were almost identical if the proportion of infected ticks was above 20% but the longer durations of vaccination begin to reduce more ticks for lower proportions of infected ticks. This means that if the proportion of infected ticks is above 20%, individuals using vaccines to reduce the number of infected ticks should expect to see the same results every year after two years; however, for lower proportions, they should see lower number of ticks each year if continuing to vaccinate at the same rate. The 20% prevalence of *B. burgdorferi* in nymphal ticks serves as a threshold such that at this point, the tick population is resistant to vaccination but the prevalence begins to approach very low values as vaccines are repeatedly used if the prevalence drops below 20%.

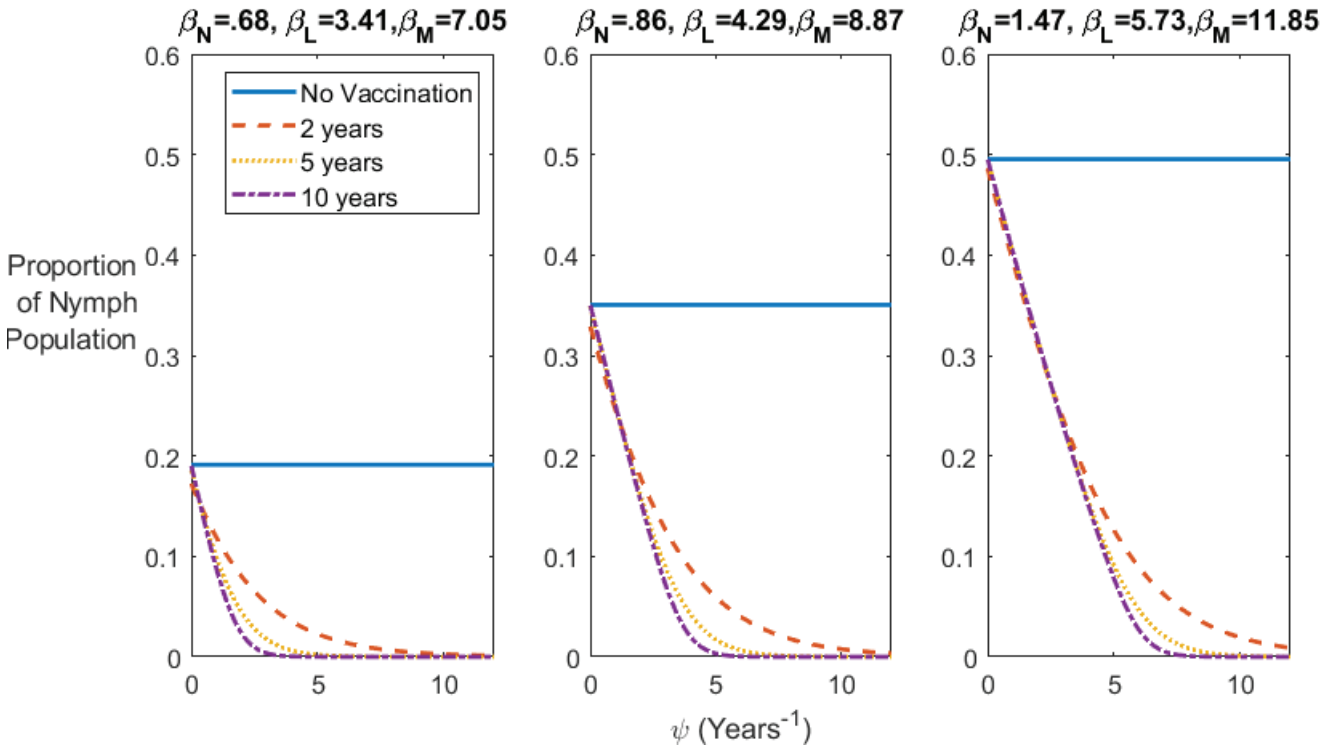

Figure 10: Vaccine effect on nymphs compared to years of use, M=50 mice, N=1000 ticks at $\mathcal{R}_C = [0.18, 3.02]$, $\mathcal{R}_C = [0.28, 4.77]$, and $\mathcal{R}_C = [0.48, 8.51]$. ($\beta_N$/yr, β_L/yr, β_M/yr)

4.3 Risk and Cost Analysis

Through risk and cost analysis we can understand the effectiveness of mice vaccination at reducing human cases of Lyme disease. We have determined that vaccines can significantly reduce the number of infected nymphal ticks in an area; thus we also compare the cost of vaccination with reductions of human risk to determine if the intervention is cost-effective. In order to predict the change in the risk of human Lyme disease cases, we construct the following function for the yearly number of new human cases, I, also known as the incidence rate:

$$I = \frac{N_I}{N} \cdot \rho \cdot \gamma \cdot H_S,$$

where ρ is the probability of infection for humans after nymph bite and γ is the biting rate of tick nymph per human per year. N_I is the number of infected nymphs dependent on ψ and β values. We did not take N_I at the fixed point because this value often took decades or centuries to reach, which would not be a feasible amount of time for this intervention. Although adult ticks also bite humans, we do not include these contacts in our model because this is minimal in terms of transmitting infection to humans; due to the large size of these ticks, most are detected and removed before the necessary time to transmit the infection [6, 27]. We take the value of ρ to be 0.031, obtained by taking an average from a range of values in our source [19]. We found γ to be valued at 0.005/day, or equivalently 0.913/year[2], from another model but decided to vary this

[2] $0.005 * 365 = 1.825$/year. Nymphs are active for only half the year, and $1.825/2 \approx 0.913$

value since it was unclear how this γ had been calculated [38].

H_S is the number of people who spend their tick exposure time in that tick-infected region. There are three components to calculating H_S. First is the yearly number of unique people that move through an area. Second is the average percentage of those people's tick exposure time spent in the vaccination area. Third is the percentage of that area that is covered by 1 hectares. For example, 1,000 unique people may walk on a suburban trail in a year. Since this a neighborhood trail, most of those people are likely regularly there walking dogs or spending time with their children so the average person may spend 80% of their total time exposed to ticks on that trail. Finally, that trail may be a kilometer long so if mice are vaccinated for 50 meters on either side of the trail, the total vaccination area would be 5 hectares so a single hectare of vaccination would only cover 20% of the total trail risk. This gives us our first estimated H_S value of 160. The other two estimated values follow similarly. One accounts for a similar trail, but less populated, and the other represents a public park. Table 4 compares these three scenarios.

H_S value	80	160	750
Geographical area	Trail	Trail	Park
Number of people	500	1000	5000
Proportion of time spent	80%	80%	30%
Proportion of area covered	20%	20%	50%

Table 4: Scenarios for estimation of H_S values

To analyze the cost of Lyme disease treatment, we examine the relationship between total cost of implementation of mice vaccination and average cost for Lyme disease treatment per infected person. We assume a linear relationship between ψ, the vaccination rate per year, and the increase in cost per increase in vaccination rate, x. Considering the fact that white-footed mice are territorial, it is possible that a particular nest of mice are the only ones feeding from a particular bait box[31]. Thus, the same amount of mice would access each box regardless of the number of boxes until all mice are vaccinated, making this assumption biologically feasible. This achieves the following cost function,

$$C_{total} = x \cdot \psi + I \cdot \theta$$

where θ is the average cost of Lyme disease treatment per infection, calculated to be \$3537.70 per year per person based on studies of health care costs of Lyme disease, as shown in Appendix 6.5. Using data from a field study of vaccines targeting white-footed mice, we estimated x to be \$329.29 per unit increase in ψ, as shown in Appendix 6.5 [14, 29]. Thus the total cost will be given by Equation (6)

$$C_{total} = x \cdot \psi + \theta \cdot \rho \cdot \gamma \cdot \frac{N_I}{N} H_S. \tag{6}$$

For a summary of parameters of the cost function as well as their definitions and values see Table 5:

PARAM	Definition	Unit	Value	Source
x	Increase in cost per increase in vaccination rate	dollars	$329.29	[29]
ψ	Contact between mice and vaccines	1/year	Estimated	-
θ	Average cost of Lyme disease treatment	dollars/infection	$3537.70	[1]
ρ	Prob. of infection for humans after nymph bite	infections/bites	.031	[19]
γ	Biting rate of tick nymph per human per year	bites/(human·year)	Estimated	-
H_S	Susceptible humans	people	Estimated	-

Table 5: Parameters values for risk and cost equations

We then modeled the relationship between vaccination rate and dollars saved in a human population infected with Lyme disease and mouse vaccination intervention after ten years across varying values of γ. Figures 11, 12, and 13 represent susceptible populations of 80, 160, and 750 humans, respectively. In all of these plots we observe a similar trend in that the higher the value of γ, the more money saved. However, only for a human population size of 1,000 does vaccination become cost-effective for every γ value. We also observe that at certain points there is an optimal value for ψ that will guarantee the most money saved. The greater the human population, the greater the vaccination rate needs to be in order to maximize cost-effectiveness. Additionally, this maximum value is much greater for larger human populations. In the parks, the highest number of susceptible humans, vaccination saved up to approximately $27,000 per year whereas significantly less money is saved from vaccinating on trails.

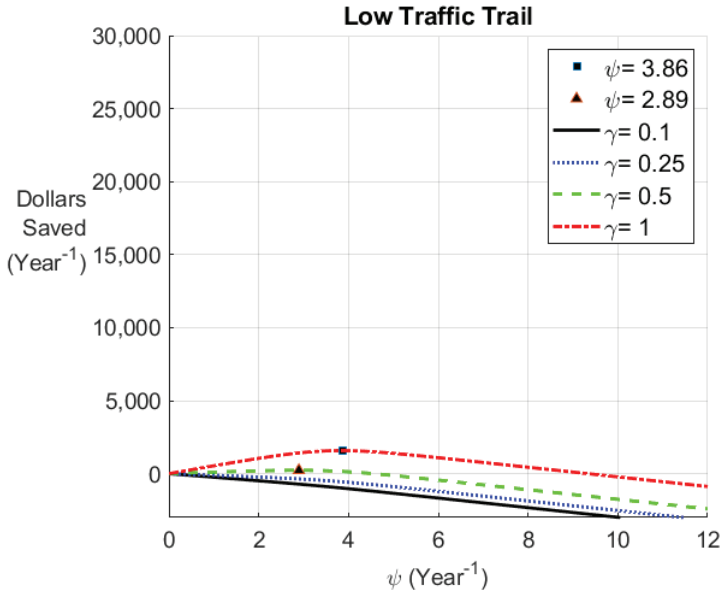

Figure 11: Dollars saved after 10 years of vaccination for varying nymphal biting rates, $H_S = 80$, M=50, N=1000, β_N=0.86/year, β_L=4.29/year, β_M=8.87/year

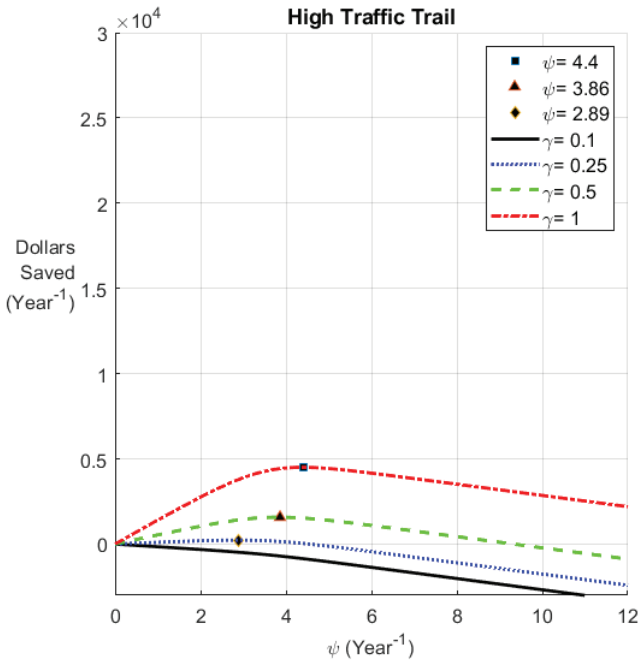

Figure 12: Dollars saved after 10 years of vaccination for varying nymphal biting rates, $H_S = 160$, M=50, N=1000, β_N=0.86/year, β_L=4.29/year, β_M=8.87/year

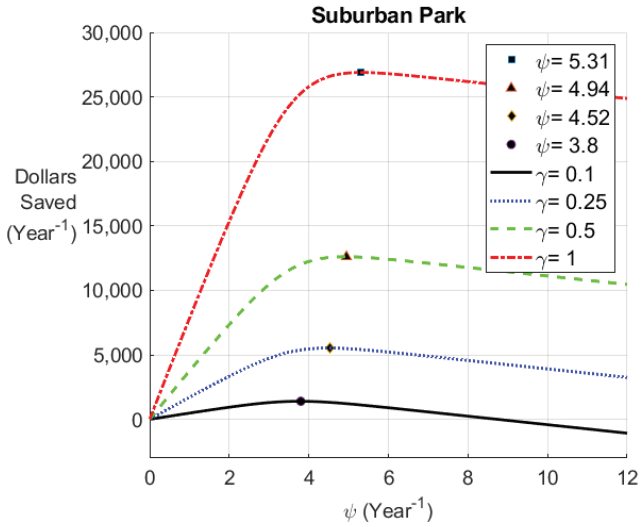

Figure 13: Dollars saved after 10 years of vaccination for varying nymphal biting rates, $H_S = 750$, M=50, N=1000, β_N=0.86/year, β_L=4.29/year, β_M=8.87/year

This reflects that vaccines can be a cost-efficient method when compared to treatment for Lyme disease but likely will only remain cost-efficient when mice are coming into frequent contact with bait boxes, especially in areas that have a high level of human traffic.

5 Discussion

In the present research, a coupled mouse ($M_S - M_I - M_V$) and nymphal tick ($N_S - N_I$) model was used to determine whether the implementation of vaccination of the mouse populations in fragmented forests could reduce the population of infected ticks there. This model captures both the seasonal dynamics of the mouse-tick interactions and the effects of vaccination on the persistence of the infection. These characteristics are important because an accurate estimate of the infection prevalence within the nymphal stage can provide a direct relationship with the expected number of human cases in an area and the cost-effectiveness of vaccines.

Preliminary analysis is based on first proving constant population size in both species to reduce the system of equations to ($M_I - M_V$) and (N_I). With our reduced system of equations the existence of solutions was tested, giving us two roots demonstrating the existence of a disease-free equilibrium and an endemic equilibrium with and without vaccination. Due to the nature of the equations, only the disease-free equilibrium could be explicitly found. Through the use of the Jacobian and a next-generation matrix approach the stability conditions and $\mathcal{R}_C$ were calculated for the disease-free equilibrium.

The results from computer simulations show that vaccination can eliminate transmission of *B. burgdorferi* between mice and ticks and can do so at achievable rates and duration of vaccination. Furthermore, we discovered that the proportion of infected ticks can be reduced to below one at vaccination rates significantly less than those required to reduce $\mathcal{R}_C$ to less than 1. This means that though $\mathcal{R}_C$ being less than one is sufficient for elimination of the tick-mouse transmission pathway, it often is not required. Additionally, we found that the vaccination rates required to reduce the number of infected ticks to 20% were the same regardless of duration of vaccination but that the duration of vaccination began to have a major impact on infected tick reduction for prevalences lower than 20%. This tells us that the proportion of infected ticks can be reduced to 20% within the first two years but long-term vaccination would likely be required to actually eliminate the transmission pathway.

Furthermore, the cost-benefit analysis shows that vaccine intervention is cost-effective if there is significant human presence in the area, and especially if there is a high rate of tick bites to these humans. In its current form, vaccination of mice may never eradicate *B. burgdorferi* worldwide since there are other reservoirs carrying the infection, but it could prove to be a cost-effective measure to reduce human cases of Lyme disease in specific targeted areas where mice are primary reservoirs. We believe this could be a particularly practical measure in fragmented forests near human settlements like parks or wooded areas in and around suburban developments. These environments often have very high infection prevalence among nymphal ticks, low mammal diversity, and high levels of human activity.

In future research, this model could be adapted to include influence of other control factors. Some promising methods include chemical or fungal pesticides to cull tick populations, or increasing mammalian biodiversity to allow for predation or for competition with less competent reservoirs of small mammal hosts. Modeling the pesticide methods could include adding classes of mice that are protected by pesticide applied directly to their fur through similar bait boxes to the ones that deliver the vaccine. Increased biodiversity might include predator-prey or competition dynamics with different species of host having different transmission rates. Any of these modifications could quickly become much more complicated as more compartments are added to the model. It would also be

possible to produce a more detailed cost analysis, perhaps with compartments for susceptible, infectious, and susceptible again, or with more intensive parameter estimation. Lyme disease is a significant public health problem, and a variety of mathematical models could offer solutions without the need for expensive field tests.

Acknowledgments

We would like to thank Dr. Carlos Castillo-Chavez, Founding and Co-Director of the Mathematical and Theoretical Biology Institute (MTBI), for giving us the opportunity to participate in this research program. We would also like to thank Co-Director Dr. Anuj Mubayi as well as Coordinator Ms. Rebecca Perlin and Management Intern Ms. Sabrina Avila for their efforts in planning and executing the day to day activities of MTBI. This research was conducted as part of 2018 MTBI at the Simon A. Levin Mathematical, Computational and Modeling Sciences Center (MCMSC) at Arizona State University (ASU). This project has been partially supported by grants from the National Science Foundation (NSF–Grant MPS-DMS-1263374 and NSF–Grant DMS-1757968), the National Security Agency (NSA–Grant H98230-J8-1-0005), the Alfred P. Sloan Foundation, the Office of the President of ASU, and the Office of the Provost of ASU.

6 Appendix

6.1 Appendix 1 - General, Discrete form of transition equations

Mice in Vaccine System		
Event	Flow	Term in Equation
Mice are born	$\rightarrow M_S$	$M_S(\tau + \frac{i+1}{k})$=$c^*\Lambda_M + M_S(\tau + \frac{i}{k})$
Mice are Vaccinated	$M_S \rightarrow M_V$	$M_S(\tau + \frac{i+1}{k}) = M_S(\tau + \frac{i}{k})e^{-c\psi\omega}$
		$V_M(\tau + \frac{i+1}{k}) = M_V(\tau + \frac{i}{k}) + M_S(\tau + \frac{i}{k})(1 - e^{-c\psi\omega})$
Mice Die	$M_S \rightarrow$	$M_S(\tau + \frac{i+1}{k}) = M_S(\tau + \frac{i}{k})e^{-c\mu}$
	$M_I \rightarrow$	$M_I(\tau + \frac{i+1}{k}) = M_I(\tau + \frac{i}{k})e^{-c\mu}$
	$M_V \rightarrow$	$M_V(\tau + \frac{i+1}{k}) = M_V(\tau + \frac{i}{k})e^{-c\mu}$
Mice are Infected	$M_S \rightarrow M_I$	$M_S(\tau + \frac{i+1}{k}) = M_S(\tau + \frac{i}{k})e^{\frac{-c\beta I_S}{N_I(\tau+\frac{i}{k})+N_S(\tau+\frac{i}{k})}}$
		$M_I(\tau + \frac{i+1}{k}) = M_I(\tau + \frac{i}{k}) + M_S(\tau + \frac{i}{k})(1 - e^{\frac{-c\beta I_S}{N_I(\tau+\frac{i}{k})+N_S(\tau+\frac{i}{k})}})$

Event	Flow	Term in Equation
Ticks Die	$L_S \rightarrow$	$L_S(\tau + \frac{i+1}{k}) = L_S(\tau + \frac{i}{k})e^{-c\alpha}$
	$N_S \rightarrow$	$N_S(\tau + \frac{i+1}{k}) = N_S(\tau + \frac{i}{k})e^{-c\alpha}$
	$N_I \rightarrow$	$N_I(\tau + \frac{i+1}{k}) = N_I(\tau + \frac{i}{k})e^{-c\alpha}$
	$A_S \rightarrow$	$A_S(\tau + \frac{i+1}{k}) = A_S(\tau + \frac{i}{k})e^{-c\alpha}$
	$A_I \rightarrow$	$A_I(\tau + \frac{i+1}{k}) = A_I(\tau + \frac{i}{k})e^{-c\alpha}$
Larvae Feed	$L_S \rightarrow N_I$	$N_I(\tau + \frac{i+1}{k}) = L_S(\tau + \frac{i}{k})e^{-c\beta_L \frac{M_I(\tau+\frac{i}{k})}{{**}M(\tau+\frac{i}{k})}}$
	$L_S \rightarrow N_S$	$N_S(\tau + \frac{i+1}{k}) = L_S(\tau + \frac{i}{k})(1 - e^{-c\beta_L \frac{M_I(\tau+\frac{i}{k})}{M(\tau+\frac{i}{k})}})$
Nymphs Feed	$N_I \rightarrow A_I$	$A_I(\tau + \frac{i+1}{k}) = N_S(\tau + \frac{i}{k})$
	$N_S \rightarrow A_I$	$A_I(\tau + \frac{i+1}{k}) = N_S(\tau + \frac{i}{k})e^{-c\beta_N \frac{M_I(\tau+\frac{i}{k})}{M(\tau+\frac{i}{k})}}$
	$N_S \rightarrow A_S$	$A_S(\tau + \frac{i+1}{k}) = N_S(\tau + \frac{i}{k})(1 - e^{-c\beta_N \frac{M_I(\tau+\frac{i}{k})}{M(\tau+\frac{i}{k})}})$
Larvae Hatch	$\rightarrow L_S$	$L_S(\tau + \frac{i+1}{k}) = L_s(\tau + \frac{i}{k}) + c\Lambda_T$

Table 6: Discrete terms associated with flow rates in the system.

*c is the proportion of the year for which the particular process takes place. This is not constant for a given compartment transition and depends on the ordering of events and transitions being divided into multiple events.
***$M(\tau) = M_I(\tau) + M_V(\tau) + M_S(\tau)$ is the total mouse population at time τ.

6.2 Appendix 2 - Model Derivation

Let $M(\tau)$= $M(\tau)$ and $N(\tau)$=$N_I(\tau) + N_S(\tau)$.

1. Mice are vaccinated

$$M_S(\tau + \frac{1}{11}) = M_S(\tau)e^{-\frac{\psi\omega}{4}}$$
$$M_V(\tau + \frac{1}{11}) = M_V(\tau) + M_S(\tau)(1 - e^{-\frac{\psi\omega}{4}})$$

2. Nymphs infect mice

$$\begin{aligned} M_S(\tau + \frac{2}{11}) &= M_S(\tau + \frac{1}{11})e^{-\frac{\beta_M}{2}\frac{N_I(\tau)}{N(\tau)}} \\ &= M_S(\tau)e^{-\frac{\psi\omega}{4}}e^{-\frac{\beta_M}{2}\frac{N_I(\tau)}{N(\tau)}} \\ M_I(\tau + \frac{2}{11}) &= M_I(\tau + \frac{1}{11}) + M_S(\tau + \frac{1}{11})\left(1 - e^{-\frac{\beta_M}{2}\frac{N_I(\tau)}{N(\tau)}}\right) \\ &= M_I(\tau) + M_S(\tau)e^{-\frac{\psi\omega}{4}}\left(1 - e^{-\frac{\beta_M}{2}\frac{N_I(\tau)}{N(\tau)}}\right) \end{aligned}$$

3. Susceptible and infected nymphs feed on mice and become infected adults

$$\begin{aligned} A_I(\tau + \frac{3}{11}) &= N_I(\tau + \frac{2}{11}) + N_S(\tau + \frac{2}{11})\left(1 - e^{-\frac{\beta_N}{2}\frac{M_I(\tau+\frac{2}{11})}{M(\tau+\frac{2}{11})}}\right) \\ &= N_I(\tau) + N_S(\tau)\left(1 - e^{-\frac{\beta_N}{2}\frac{M_I(\tau)+M_S(\tau)e^{-\frac{\psi\omega}{4}}\left(1-e^{-\frac{\beta_M}{2}\frac{N_I(\tau)}{N(\tau)}}\right)}{M(\tau)}}\right) \end{aligned}$$

Susceptible nymphs become susceptible adults

$$\begin{aligned} A_S(\tau + \frac{3}{11}) &= N_S(\tau + \frac{2}{11})\left(e^{-\frac{\beta_N}{2}\frac{M_I(\tau+\frac{2}{11})}{M(\tau+\frac{2}{11})}}\right) \\ &= N_S(\tau)(e^{-\frac{3\alpha_3}{4}})\left(e^{-\frac{\beta_N}{2}\frac{M_I(\tau)+M_S(\tau)e^{-\frac{\psi\omega}{4}}\left(1-e^{-\frac{\beta_M}{2}\frac{N_I(\tau)}{N(\tau)}}\right)}{M(\tau)}}\right) \end{aligned}$$

4. Mice die

$$\begin{aligned}
M_S(\tau+\frac{4}{11}) &= M_S(\tau+\frac{3}{11})e^{-\frac{\mu}{4}} \\
&= M_S(\tau)e^{-\frac{\mu}{4}}e^{-\frac{\psi\omega}{4}}e^{-\frac{\beta_M}{2}\frac{N_I(\tau)}{N(\tau)}} \\
M_I(\tau+\frac{4}{11}) &= M_I(\tau+\frac{3}{11})e^{-\frac{\mu}{4}} \\
&= M_I(\tau)e^{-\frac{\mu}{4}} + M_S(\tau)e^{-\frac{\mu}{4}}e^{-\frac{\psi\omega}{4}}\left(1-e^{-\frac{\beta_M}{2}\frac{N_I(\tau)}{N(\tau)}}\right) \\
M_V(\tau+\frac{4}{11}) &= M_V(\tau+\frac{3}{11})e^{-\frac{\mu}{4}} \\
&= M_V(\tau)e^{-\frac{\mu}{4}} + M_S(\tau)e^{-\frac{\mu}{4}}(1-e^{-\frac{\psi\omega}{4}})
\end{aligned}$$

5. Mice are born

$$\begin{aligned}
M_S(\tau+\frac{5}{11}) &= M_S(\tau+\frac{4}{11}) + \frac{\Lambda_M}{4} \\
&= M_S(\tau)e^{-\frac{\mu}{4}}e^{\frac{-\psi\omega}{4}}e^{-\frac{\beta_M}{2}\frac{N_I(\tau)}{N(\tau)}} + \frac{\Lambda_M}{4}
\end{aligned}$$

6. Larvae hatch

$$\begin{aligned}
L_S(\tau+\frac{6}{11}) &= L_S(\tau+\frac{5}{11}) + \Lambda_T \\
&= \Lambda_T
\end{aligned}$$

7. Larvae Die

$$\begin{aligned}
L_S(\tau+\frac{7}{11}) &= L_S(\tau+\frac{6}{11})e^{\frac{-\alpha_1}{4}} \\
&= e^{-\frac{\alpha_1}{4}}\Lambda_T
\end{aligned}$$

8. Larvae feed, possibly get infected, and transition to nymphs

$$N_S(\tau+\frac{8}{11}) = L_S(\tau+\frac{7}{11})\left(e^{-\frac{\beta_L}{4}\frac{M_I(\tau+\frac{7}{11})}{M(\tau+\frac{7}{11})}}\right)$$
$$= \Lambda_T e^{-\frac{\alpha_1}{4}}\left(e^{-\frac{\beta_L}{4}\frac{M_I(\tau)e^{-\frac{\mu}{4}}+M_S(\tau)e^{-\frac{\mu}{4}}e^{-\frac{\psi\omega}{4}}\left(1-e^{-\frac{\beta_M}{2}\frac{N_I(\tau)}{N(\tau)}}\right)}{e^{-\frac{\mu}{4}}M(\tau)+\frac{\Lambda_M}{4}}}\right)$$

$$N_I(\tau+\frac{8}{11}) = L_S(\tau+\frac{7}{11})\left(1-e^{-\frac{\beta_L}{4}\frac{M_I(\tau+\frac{7}{11})}{M(\tau+\frac{7}{11})}}\right)$$
$$= \Lambda_T e^{-\frac{\alpha_1}{4}}\left(1-e^{-\frac{\beta_L}{4}\frac{M_I(\tau)e^{-\frac{\mu}{4}}+M_S(\tau)e^{-\frac{\mu}{4}}e^{-\frac{\psi\omega}{4}}\left(1-e^{-\frac{\beta_M}{2}\frac{N_I(\tau)}{N(\tau)}}\right)}{e^{-\frac{\mu}{4}}M(\tau)+\frac{\Lambda_M}{4}}}\right)$$

9. Nymphs die

$$N_S(\tau+\frac{9}{11}) = N_S(\tau+\frac{8}{11})e^{-\frac{3\alpha_2}{4}}$$
$$= \Lambda_T e^{-\frac{(\alpha_1+3\alpha_2)}{4}}\left(e^{-\frac{\beta_L}{4}\frac{M_I(\tau)e^{-\frac{\mu}{4}}+M_S(\tau)e^{-\frac{\mu}{4}}e^{-\frac{\psi\omega}{4}}\left(1-e^{-\frac{\beta_M}{2}\frac{N_I(\tau)}{N(\tau)}}\right)}{e^{-\frac{\mu}{4}}M(\tau)+\frac{\Lambda_M}{4}}}\right)$$

$$N_I(\tau+\frac{9}{11}) = N_I(\tau+\frac{8}{11})e^{-\frac{3\alpha_2}{4}}$$
$$= \Lambda_T e^{-\frac{(\alpha_1+3\alpha_2)}{4}}\left(1-e^{-\frac{\beta_L}{4}\frac{M_I(\tau)e^{-\frac{\mu}{4}}+M_S(\tau)e^{-\frac{\mu}{4}}e^{-\frac{\psi\omega}{4}}\left(1-e^{-\frac{\beta_M}{2}\frac{N_I(\tau)}{N(\tau)}}\right)}{e^{-\frac{\mu}{4}}M(\tau)+\frac{\Lambda_M}{4}}}\right)$$

10. Mice die

$$\begin{aligned}
M_S(\tau+\frac{10}{11}) &= M_S(\tau+\frac{9}{11})e^{-\frac{3\mu}{4}} \\
&= M_S(\tau)e^{-\mu}e^{-\frac{\psi\omega}{4}}e^{-\frac{\beta_M}{2}\frac{N_I(\tau)}{N(\tau)}} + \frac{\Lambda_M}{4}e^{-\frac{3\mu}{4}} \\
M_I(\tau+\frac{10}{11}) &= M_I(\tau)e^{-\mu} + M_S(\tau)e^{-\mu}e^{-\frac{\psi\omega}{4}}(1-e^{-\frac{\beta_M}{2}\frac{N_I(\tau)}{N(\tau)}}) \\
M_V(\tau+\frac{10}{11}) &= M_V(\tau)e^{-\mu} + M_S(\tau)e^{-\mu}(1-e^{-\frac{3\mu}{4}})
\end{aligned}$$

11. Mice are born

$$\begin{aligned}
M_S(\tau+1) &= M_S(\tau)e^{-\mu}e^{-\frac{\psi\omega}{4}}e^{-\frac{\beta_M}{2}\frac{N_I(\tau)}{N(\tau)}} + \frac{\Lambda_M}{4}e^{-\frac{3\mu}{4}} + \frac{3\Lambda_M}{4} \\
&= M_S(\tau)e^{-\mu}e^{-\frac{\psi\omega}{4}}e^{-\frac{\beta_M}{2}\frac{N_I(\tau)}{N(\tau)}} + \frac{\Lambda_M}{4}(e^{-\frac{3\mu}{4}}+3)
\end{aligned}$$

12. Final equations

$$N_I(\tau+1) = \Lambda_T e^{-\frac{(\alpha_1+3\alpha_2)}{4}}\left(1-e^{-\frac{\beta_L}{4}\frac{M_I(\tau)e^{-\frac{\mu}{4}}+M_S(\tau)e^{-\frac{\mu}{4}}e^{-\frac{\psi\omega}{4}}\left(1-e^{-\frac{\beta_M}{2}\frac{N_I(\tau)}{N(\tau)}}\right)}{e^{-\frac{\mu}{4}}M(\tau)+\frac{\Lambda_M}{4}}}\right)$$

$$N_S(\tau+1) = \Lambda_T e^{-\frac{(\alpha_1+3\alpha_2)}{4}}\left(e^{-\frac{\beta_L}{4}\frac{M_I(\tau)e^{-\frac{\mu}{4}}+M_S(\tau)e^{-\frac{\mu}{4}}e^{-\frac{\psi\omega}{4}}\left(1-e^{-\frac{\beta_M}{2}\frac{N_I(\tau)}{N(\tau)}}\right)}{e^{-\frac{\mu}{4}}M(\tau)+\frac{\Lambda_M}{4}}}\right)$$

$$\begin{aligned}
M_S(\tau+1) &= M_S(\tau)e^{-\mu}e^{-\frac{\psi\omega}{4}}e^{-\frac{\beta_M}{2}\frac{N_I(\tau)}{N(\tau)}} + \frac{\Lambda_M}{4}(e^{-\frac{3\mu}{4}}+3) \\
M_I(\tau+1) &= M_I(\tau)e^{-\mu} + M_S(\tau)e^{-\mu}e^{-\frac{\psi\omega}{4}}\left(1-e^{-\frac{\beta_M}{2}\frac{N_I(\tau)}{N(\tau)}}\right) \\
M_V(\tau+1) &= M_V(\tau)e^{-\mu} + M_S(\tau)e^{-\mu}(1-e^{-\frac{\psi\omega}{4}})
\end{aligned}$$

6.3 Appendix 3: Analysis

1. Total mouse population constant year-to-year

$$\begin{aligned} M(\tau) &= M_S(\tau+1) + M_I(\tau+1) + M_V(\tau+1) \\ &= M_S(\tau)e^{-\mu}e^{-\frac{\psi\omega}{4}}e^{-\frac{\beta_M}{2}\frac{N_I(\tau)}{N(\tau)}} + \frac{\Lambda_M}{4}(e^{-\frac{3\mu}{4}}+3)+ \\ & M_I(\tau)e^{-\mu} + M_S(\tau)e^{-\mu}e^{-\frac{\psi\omega}{4}}\left(1-e^{-\frac{\beta_M}{2}\frac{N_I(\tau)}{N_S(\tau)+N_S(\tau)}}\right)+ \\ & M_V(\tau)e^{-\mu} + M_S(\tau)e^{-\mu}\left(1-e^{-\frac{\psi\omega}{4}}\right) \\ M(\tau) &= e^{-\mu}\left(M(\tau) + \frac{\Lambda_m}{4}e^{\frac{\mu}{4}} + \frac{3}{4}e^{\mu}\Lambda_M\right) \end{aligned}$$

$$\text{Equilibrium Solution} : M(\tau) = \frac{\Lambda_M}{4}\frac{e^{\frac{-3\mu}{4}}+3}{1-e^{-\mu}}$$

2. Total nymph population constant year-to-year

$$\begin{aligned} N(\tau) &= N_S(\tau+1) + N_I(\tau+1) \\ &= \Lambda_T e^{-\frac{(\alpha_1+3\alpha_2)}{4}}\left(e^{-\frac{\beta_L}{4}\frac{M_I(\tau)e^{-\frac{\mu}{4}}+M_S(\tau)e^{-\frac{\mu}{4}}e^{-\frac{\psi\omega}{4}}\left(1-e^{-\frac{\beta_M}{2}\frac{N_I(\tau)}{N(\tau)}}\right)}{e^{-\frac{\mu}{4}}[M_I(\tau)+M_S(\tau)+M_V(\tau)]+\frac{\Lambda_M}{4}}}\right) \\ &+ \Lambda_T e^{-\frac{(\alpha_1+3\alpha_2)}{4}}\left(1-e^{-\frac{\beta_L}{4}\frac{M_I(\tau)e^{-\frac{\mu}{4}}+M_S(\tau)e^{-\frac{\mu}{4}}e^{-\frac{\psi\omega}{4}}\left(1-e^{-\frac{\beta_M}{2}\frac{N_I(\tau)}{N(\tau)}}\right)}{e^{-\frac{\mu}{4}}[M_I(\tau)+M_S(\tau)+M_V(\tau)]+\frac{\Lambda_M}{4}}}\right) \\ &= \Lambda_T e^{-\frac{(\alpha_1+3\alpha_2)}{4}} \end{aligned}$$

3. Disease-Free Equilibrium

With Vaccination

$$
\begin{aligned}
N_I(\tau) &= 0 \\
N_S(\tau) &= \Lambda_T e^{-\frac{(\alpha_1+3\alpha_2)}{4}} \\
M_I(\tau) &= 0 \\
M_S(\tau) &= \frac{\Lambda_M}{4} \frac{\left(e^{\frac{-3\mu}{4}}+3\right)}{\left(1-e^{-\mu-\frac{\psi\omega}{4}}\right)} \\
M_V(\tau) &= \frac{\Lambda_M}{4} \frac{\left(e^{\frac{\mu}{4}}+3e^{\mu}\right)\left(1-e^{\frac{\psi\omega}{4}}\right)}{(-1+e^{\mu})\left(-1+e^{\mu+\frac{\psi\omega}{4}}\right)}
\end{aligned}
$$

Without Vaccination

$$
\begin{aligned}
N_I(\tau) &= 0 \\
N_S(\tau) &= \Lambda_T e^{-\frac{(\alpha_1+3\alpha_2)}{4}} \\
M_I(\tau) &= 0 \\
M_S(\tau) &= \frac{\Lambda_M}{4} \frac{\left(e^{\frac{-3\mu}{4}}+3\right)}{(1-e^{-\mu})} \\
M_V(\tau) &= 0
\end{aligned}
$$

6.4 Appendix 4: Existence of Solution Equation

$$
\begin{aligned}
M_I^* &= M_I^* e^{-\mu} + (M_0 - M_V^* - M_I^*) e^{-\mu} e^{-\frac{\psi\omega}{4}} \left(1 - e^{-\frac{\beta_M}{2}\frac{N_I^*}{N_0}}\right) \\
M_V^* &= M_V^* e^{-\mu} + (M_0 - M_V^* - M_I^*) e^{-\mu} (1 - e^{-\frac{\psi\omega}{4}}) \\
N_I^* &= N_0 \left(1 - e^{-\frac{\beta_L}{4} \frac{M_I^* e^{-\frac{\mu}{4}} + (M_0 - M_V^* - M_I^*) e^{-\frac{\mu}{4}} e^{-\frac{\psi\omega}{4}} \left(1 - e^{-\frac{\beta_M}{2}\frac{N_I^*}{N_0}}\right)}{e^{-\frac{\mu}{4}} M_0 + \frac{\Lambda_M}{4}}} \right)
\end{aligned}
$$

Solving equation 2 for M_V^* in terms of M_I^*.

$$M_V^* = M_V^* e^{-\mu} + (M_0 - M_V^* - M_I^*)e^{-\mu}(1 - e^{-\frac{\psi\omega}{4}})$$

$$M_V^*(M_I^*) = \frac{\left(-1 + e^{\frac{\psi\omega}{4}}\right)(M_0 - M_I^*)}{\left(-1 + e^{\mu + \frac{\psi\omega}{4}}\right)}$$

Solving equation 1 for M_I^* in terms of N_I^*.

$$M_I^* = M_I^* e^{-\mu} + (M_0 - M_V^* - M_I^*)e^{-\mu}e^{-\frac{\psi\omega}{4}}\left(1 - e^{-\frac{\beta_M}{2}\frac{N_I^*}{N_0}}\right)$$

$$M_I^*(N_I^*) = \frac{\left(-1 + e^{\frac{N_I^*\beta}{2N_0}}\right)M_0}{-1 + e^{\frac{N_I^*\beta}{2N_0} + \mu + \frac{\psi\omega}{4}}}$$

Solving equation 3 in terms of N_I^*.

$$N_I^* = N_0\left(1 - e^{-\frac{\beta_L}{4}\frac{M_I^* e^{-\frac{\mu}{4}} + (M_0 - M_V^* - M_I^*)e^{-\frac{\mu}{4}}e^{-\frac{\psi\omega}{4}}\left(1 - e^{-\frac{\beta_M}{2}\frac{N_I^*}{N_0}}\right)}{e^{-\frac{\mu}{4}}M_0 + \frac{\Lambda_M}{4}}}\right)$$

$$G(N_I^*) = \ln\left(1 - \frac{N_I^*}{N_0}\right) + \frac{\beta_L M_0 e^{\frac{-\mu}{4}}e^{-\frac{\psi\omega}{4}}}{4\left(e^{\frac{-\mu}{4}}M_0 + \frac{\Lambda_M}{4}\right)}\left(\frac{1 - e^{\frac{-\beta_M}{2}\frac{N_I^*}{N_0}}}{1 - e^{-\mu}e^{\frac{-\psi\omega}{4}}e^{\frac{-\beta_M}{2}\frac{N_I^*}{N_0}}}\right) = 0$$

6.5 Appendix 5: Parameter Estimation

- Calculation of α_1, α_2, α_3: Using data from literature, we used survival proportions of 0.05, 0.1, and 0.2 between each stage of the tick life cycle and calculated the α values based on the proportions of death that we considered in our model [36].

  α_1: Egg to larva

$$\begin{aligned} e^{-\frac{\alpha_1}{4}} &= 0.05 \\ -\frac{\alpha_1}{4} &= \ln(0.05) \\ \alpha_1 &= -4\ln(0.05) \\ &= 11.98 \end{aligned}$$

α_2: Larva to nymph

$$\begin{aligned} e^{-\frac{3\alpha_2}{4}} &= .1 \\ \alpha_2 &= -\frac{4}{3}\ln(0.1) \\ &= 3.07 \end{aligned}$$

α_3: Nymph to adult

$$\begin{aligned} e^{-\frac{\alpha_3}{2}} &= 0.2 \\ \alpha_3 &= 2\ln(0.2) \\ &= 3.22 \end{aligned}$$

- Calculation of Λ_M: Using $M(\tau)$ from our equilibrium solution in Appendix 6.3 and the chosen value for the total mice population $M(\tau)$= 50, along with $\mu = 4.38$, we have

$$50 = \frac{\Lambda_M}{4}\frac{e^{\frac{-3(4.38)}{4}} + 3}{1 - e^{-4.38}}$$

  and thus $\Lambda_M = 65.02$.

- Calculation of Λ_T: Using $M(\tau)$ from our equilibrium solution in Appendix 6.3 and the chosen value for the total mice population $N(\tau)$= 1000, along with $\alpha_1 = 11.98$ and $\alpha_2 = 3.07$, we have

$$1000 = \Lambda_T e^{-\frac{(11.98+3\cdot 3.07)}{4}}$$

  and thus $\Lambda_T = 1.998$ x 10^5.

- Estimation of ω: We obtained this value from a study that evaluated vaccines in mice, specifically ones that included the same surface protein that we looked into for this study and corresponded with the field trial that we referenced throughout[29, 35]. Though the paper had multiple values for effectiveness, we used the ω that corresponded to 100 ng vaccine; this value was presented as a proportion and thus no conversion of units was needed.

- Calculation of μ: From literature, we found that the natural death rate of mice was .012/day. Thus, we multiplied by 365 to obtain the yearly value of 4.38/year.

- Calculation of x: The cost of increasing the vaccination rate by 1/day, is estimated by analysis of field data from a vaccine field trial [29]. The following data points were used.

1. White-Footed mouse captures
   We took data from Table 1: Number of White-Foot Mouse (WFM) Captures in the Field, recreated below.

Study Year	Unique WFM Captured	Nights of Trap Use	Total WFM Captures	WFM Trapability
2007	700	9472	6043	8.63
2008	240	13824	1647	6.86
2009	716	26112	5399	7.75
2010	877	27136	3806	4.83
2011	1258	24064	6078	4.83
Overall	3791	100608	22973	6.48

2. Plots per year
   The field trial also used 64 traps per 1.1 hectare plot for distributing vaccines or as controls and used the following number of plots every year.

Year	2007	2008	2009	2010	2011
Plots Used	4	5	7	7	7

Using this data we construct the following equation for bait-box contact rate in a year. Due to the high average captures per mouse we assume that the unique number of mice captured provides a good estimate to the number of mice in all the plots.

$$B(t) = \frac{\text{Total WFM Captures}}{\text{Nights of Trap Use}} * 64 \frac{\text{Number of Plots Used}}{\text{Unique WFM Captured}}$$

We average $B(t)$ across the five study years to obtain $B_{Mean} = .1366$ per day. The study achieved successful vaccination in a mouse after approximately 5 captures so we estimate the study's vaccination rate, $\psi = \frac{B_{Mean}}{5} = .02732/\text{day} = 9.9718/\text{year}$. We assume the cost of a bait box distributing vaccine to be equal to a bait box distributing acaricide which are on average priced at \$50 per box per year [14]. The cost to vaccinate 1.1 hectares at a rate $\psi = 9.9718$ is calculated by $\frac{\$50 * 64}{\text{year}} = \frac{\$3200}{\text{year}}$. We then solve for x:

$$\begin{aligned} C_{Vaccination} &= x * \psi \\ 3200 &= x \cdot 9.718 \\ x &= \$329.29. \end{aligned}$$

- Calculation of θ: From values from a study on health care costs of Lyme disease, we used the following equation[1]:

$$\begin{aligned} \theta = & \begin{array}{l}\text{health care costs}\\ \text{for an acute case of}\\ \text{Lyme disease}\end{array} + \begin{array}{l}\text{probability of developing}\\ \text{Post-Treatment}\\ \text{Lyme Disease Syndrome}\end{array} * \begin{array}{l}\text{average yearly}\\ \text{cost of PTLDS}\end{array} \\ = & \$2,968 + .15(\$3,798) \\ = & \$3537.70 \end{aligned}$$

Probability of .15 was taken from the same source as an average of the range of probabilities of developing PTLDS (10%-20%).

- Calculation of ρ: The source cites the probability of Lyme disease after a tick bite to be from .012 to .05[19]. Averaging these two values gives .031 for our ρ value.

References

[1] Adrion E.R., Aucott J.,Lemke K.W., Weiner J.P. Health Care Costs, Utilization and Patterns of Care following Lyme Disease. *PLOS ONE*, 10(2):1–14, 02 2015.

[2] Allan B.F. and Keesing F. and Ostfeld R.S. Effect of forest fragmentation on lyme disease risk. *Conservation Biology*, 17(1):267–272.

[3] Allen L.J.S., van den Driesscheb P. The basic reproduction number in some discrete-time epidemic models. *Journal of Difference Equations and Applications*, 14(11), October-November 2008.

[4] Barbour A.G. and Fish D. The Biological and Social Phenomenon of Lyme Disease. *Science*, 260(5114):1610–1616, 1993.

[5] Barbour A.G., Bunikis J., Fish D., and Hanincová K. Association between body size and reservoir competence of mammals bearing *Borrelia burgdorferi* at an endemic site in the north-eastern United States. *Parasites & Vectors*, 8(1):299, May 2015.

[6] Caraco T., Glavanakov S., Chen G., Flaherty J.E., Ohsumi T.K., Szymanski B.K. Stage-Structured Infection Transmission and a Spatial Epidemic: A Model for Lyme Disease. *The American Naturalist*, 160(3):348–359, 2002. PMID: 18707444.

[7] Cook M.J. Lyme *borreliosis*: a review of data on transmission time after tick attachment. *International Journal of General Medicine*, 8:1–8.

[8] Cornstedt P., Shueler W., Meinke A., Lundber U. The novel Lyme *borreliosis* vaccine VLA15 shows broad protection against *Borrelia* species expressing six different OspA serotypes. *PLoS One*, 10(9), 2017.

[9] Dobson A.D.M, Finnie T.J.R, Randolph S.E. A modified matrix model to describe the seasonal population ecology of the European tick *Ixodes ricinus*. *Journal of Applied Ecology*, 48(4):1017–1028, 2011.

[10] Moreno-Cid J. et.al. Control of multiple arthropod vector infestations with subolesin/akirin vaccines. *Vaccine*, (8), 2013.

[11] Centers for Disease Control and Prevention. How many people get Lyme disease? https://www.cdc.gov/lyme/stats/humancases.html. Accessed: 2018-07-06.

[12] Centers for Disease Control and Prevention. Lyme disease. https://www.cdc.gov/lyme/index.html, January 2018. Accessed: 2018-7-11.

[13] Hersh M.J, et. al. When is a parasite not a parasite? effects of larval tick burdens on white-footed mouse survival. *Ecology*, 95(5):1360–1369, 2014.

[14] Interland J. Bait Boxes Are a Safe Way to Keep Ticks Out of Your Yard. https://www.consumerreports.org/pest-control/bait-boxes-are-a-safe-way-to-keep-ticks-out-of-your-yard/, January 2018. Accessed: 2018-7-18.

[15] Izac JR, Oliver LD, Earnhart CG, Marconi RT. Identification of a defined linear epitope in the OspA protein of the Lyme disease spirochetes that elicits bactericidal antibody responses: Implications for vaccine development. *Vaccine*, (35(24) p.3178-3185), 2017.

[16] Jordan R.A, Schulze T.L, Jahn, M.B. Effects of Reduced Deer Density on the Abundance of *Ixodes scapularis* (*Acari: Ixodidae)* and Lyme Disease Incidence in a Northern New Jersey Endemic Area. *Journal of Medical Entomology*, 44(5):752–757, 2007.

[17] Lane R S, Piesman J and Burgdorfer, W. Lyme *Borreliosis*: Relation of Its Causative Agent to Its Vectors and Hosts in North America and Europe. *Annual Review of Entomology*, 36(1):587–609, 1991. PMID: 2006870.

[18] LoGiudice K. , et. al. The ecology of infectious disease: Effects of host diversity and community composition on Lyme disease risk. *National Academy of Sciences*, (vol. 100 no. 2 567-571), 2003.

[19] Magid D., Schwartz B., Craft J., Schwartz J.S. Prevention of Lyme Disease after Tick Bites. *New England Journal of Medicine*, 327(8):534–541, 1992. PMID: 1298217.

[20] Mather T.N., Telford S.R, Adler G.H. Absence of Transplacental Transmission of Lyme Disease Spirochetes from Reservoir Mice (*Peromyscus leucopus*) to Their Offspring. *The Journal of Infectious Diseases*, 164(3):564–567, 1991.

[21] Nupp T.E. and Swihart R.K. Effect of forest patch area on population attributes of white-footed mice *(Peromyscus leucopus)* in fragmented landscapes. *Canadian Journal of Zoology*, 74(3):467–472, 1996.

[22] Minnesota Department of Health. Tickborne diseases. http://www.health.state.mn.us/divs/idepc/dtopics/tickborne/ticks.html. Accessed: 2018-07-11.

[23] Ogden N.H., Bigras-Poulin M., O'Callaghan C.J., Barker I.K., Kurtenbach K., Lindsay L.R., Charron D.F. Vector seasonality, host infection dynamics and fitness of pathogens transmitted by the tick *Ixodes scapularis*. *Parasitology*, 134(2):209–227, 2007.

[24] Ogden N.H., Bigras-Poulin M., O'Callaghan C.J., Barker I.K., Lindsay L.R., Maarouf A., Smoyer-Tomic K.E., Waltner-Toews D., Charron D.F. A dynamic population model to investigate effects of climate on geographic range and seasonality of the tick *Ixodes scapularis*. *Int. J. Parasitol*, (35, p. 275-389), 2005.

[25] Ostfeld R. and Brunner J. Climate change and *Ixodes* tick-borne diseases of humans. *Phil. Trans. R. Soc*, 370, 02 2015.

[26] Ostfeld R. S., Keesing F. Biodiversity and Disease Risk: the Case of Lyme Disease. *Conservation Biology*, 14(3):722–728, 6 2000.

[27] Ostfeld R.S., Cepeda O.M., Hazler K.R., Miller M.C. Ecology of Lyme Disease: Habitat Associations of Ticks (*Ixodes Scapularis*) In a Rural Landscape. *Ecological Applications*, 5(2):353–361, 1995.

[28] Pugliese A., Rosa R. Effect of host populations on the intensity of ticks and the prevalence of tick-borne pathogens: How to interpret the results of deer exclosure experiments. *Parasitology*, (13):1531–1544, 2008.

[29] Richer L.M., Brisson D., Melo R., Ostfeld R.S., Zeidner N., Gomes-Solecki M. Reservoir Targeted Vaccine Against *Borrelia burgdorferi*: A New Strategy to Prevent Lyme Disease Transmission. *The Journal of Infectious Diseases*, (209(12), p. 1972-1980), 2014.

[30] Rosa R., Pugliese A. Effects of tick population dynamics and host densities on the persistence of tick-borne infections. *Mathematical Biosciences*, (208(1), pp.216-240), 2007.

[31] Aguilar S. *Peromyscus leucopus* white-footed mouse. http://animaldiversity.org/accounts/Peromyscus_leucopus/, January 2018. Accessed: 2018-7-18.

[32] Schulze T., Jordan R., Williams M, Dolan M. Evaluation of the SELECT Tick Control System (TCS), a Host-Targeted Bait Box, to Reduce Exposure to *Ixodes scapularis* (*Acari: Ixodidae*) in a Lyme Disease Endemic Area of New Jersey. *Journal of Medical Entomology*, (p. 1-6), 2017.

[33] Schwan T.G. , Burgdorfer W., Schrumpf M.E., and Karstens R.H. The urinary bladder, a consistent source of *Borrelia burgdorferi* in experimentally infected white-footed mice (*Peromyscus leucopus*). *Journal of Clinical Microbiology*, 26(5):893–895, May 1988.

[34] Schwartz A.M., Hinckley A.F., Mead P.S., Hook S.A., Kugeler K.J. Surveillance for Lyme Disease — United States, 2008–2015. *MMWR Surveill Summ 2017*, (66(No. SS-22):1–12), 1992-2006.

[35] Schwendinger M.G., O'Rourke M., Traweger A., Savidis-Dacho H. AND Pilz A., Portsmouth D., Livey I., Barrett P.N., Crowe B.A. Evaluation of OspA Vaccination-Induced Serological Correlates of Protection against Lyme *Borreliosis* in a Mouse Model. *PLOS ONE*, 8(11):1–8, 11 2013.

[36] Randolph S.E. Ticks are not insects: Consequences of contrasting vector biology for transmission potential. *Parasitology Today*, (14(5) pp.186-192), 1998.

[37] Voordouw MJ, Lachish S, Dolan MC. The Lyme Disease Pathogen Has No Effect on the Survival of Its Rodent Reservoir Host. *PLOS ONE*.

[38] Wang X., Zhao X.Q. Dynamics of a Time-Delayed Lyme Disease Model with Seasonality. *SIAM Journal on Applied Dynamical Systems*, (16(2), pp. 853-881), 2017.

[39] Way J.G. and White B.N. Coyotes, Red Foxes, and the Prevalence of Lyme Disease. *Northeastern Naturalist*, 20(4):655–665.

[40] Zhang Y., Zhao X.Q. A Reaction-Diffusion Lyme Disease Model with Seasonality. *SIAM Journal on Applied Mathematics*, (73(6), pp.2077-2099), 2013.